Addis Ababa University

Addis Ababa Institute of Technology

School of Mechanical & Industrial Engineering

Modeling the Interfacial Shear Strength of Natural Fibers Epoxy Matrix by Pullout Failure Mode

A Thesis Submitted to Graduate School of Addis Ababa Institute of Technology in partial fulfillment of the requirements for the Degree of Master of Science in Mechanical Engineering

By

Fasil Henok

Advisor: Samuel Tesfaye (Ph.D.)

2022 G.C.

Declaration

I hereby declare that the work which is being presented in this thesis entitled "Modeling The Interfacial Shear Strength of Natural Fibers Epoxy Matrix By Pullout Failure Mode" is original work of my own, has not been presented for a degree of any other university and all the resource of materials used for this thesis have been duly acknowledged.

Fasil Henok Abebe

Signature: _____ Date: _____

This thesis has been submitted for examination and signed by:

Advisor: **Samuel Tesfaye (Ph.D)** Signature_____Date_____

Addis Ababa University
Institute of Technology (AAiT)
School of Mechanical and Industrial Engineering

M.Sc. Final Thesis Approval

Submitted By:

Fasil Henok _____ _____

Student Name Signature Date

Recommended By:

Samuel Tesfaye (PhD) _____ _____

Advisor Signature Date

Examined By:

Haileleoul Sahle (PhD) _____ _____

Internal Examiner Signature Date

Araya Abera (PhD) _____ _____

External Examiner Signature Date

Approved By:

Araya Abera (PhD) _____ _____

Chair Signature Date

Endorsed by:

Yilma Tadesse (PhD) _____ _____

Dean Signature Date

Ermiyas Tesfaye (PhD) _____ _____

Associate Director, Signature Date

Post graduate program

TABLE OF CONTENTS

LIST OF FIGURES

LIST OF TABLES

ABBREVIATIONS AND SYMBOLS

NF	Natural Fiber
NFC	Natural Fiber Composite
NFEM	Natural Fiber Epoxy Matrix
NFEI	Natural Fiber Epoxy Interface
CM	Composite Material
IFSS	Interfacial Shear Strength
Ø	Diameter
CE	Cohesive Element
EL	Embedded Length
CAE	Complete Abaqus Environment
FEA	Finite Element Analysis
NA	Not Available

ACKNOWLEDGMENT

First and foremost, praises and thanks to God, the Almighty, for His showers of blessings throughout my research work to complete the research successfully.

I would like to express my deepest and heartfelt thanks to my Advisor Dr. Samuel Tesfaye, for his valuable comment which contributes much to the quality of my work and provides invaluable guidance throughout this research.

My deepest appreciation also goes to my families, friends, and Teachers. I want to thank all the staff members of Addis Abba Institute of Technology School of Mechanical and Industrial Engineering. Especially I want to thank Mechanical Design Chair Dr. Araya for his support and encouragement.

ABSTRACT

Recently natural fiber composites are overtaking the place of synthetic fiber composites for many applications, so it seems crucial to model interfacial shear strength of it and study the load transfer efficiency between the fiber and the resin, which plays a significant role in determining the mechanical properties of the fiber reinforcement which the is fiber-epoxy matrix. In this paper two fiber; Pineapple fiber and kapok, which has the highest and lowest young's modulus are chosen. Twelve models, six for each kind of fiber, are developed using ABAQUS software considering different conditions, such as various fiber embedment lengths, fiber diameter, and void sizes for fiber pullout failure of the interface between the fibers and epoxy. Parameters studied are fiber embedded length of 3 mm and 0.1 mm; fiber diameter 48 μm for pineapple and Kapok fiber with a length of 1mm and 0.1 mm with a diameter of 33 μm is taken. The effect of the presence of voids on the interface of fiber and epoxy is studied. The average interfacial shear strength obtained, between epoxy and fiber interface, are $1.4016\ \mathrm{MPa}$ for pineapple and $0.0208\ \mathrm{MPa}$ for kapok. This study shows the interfacial shear strength is dependent on the elastic modulus and density of the fiber but the change in the interfacial contact surface area due to change in embedded length of fiber has no significant effect on the interfacial shear strength value. But the change in diameter of the fiber and void ratio affects interfacial shear strength. Rather the presence of void does have a positive effect on the incremental of the value interfacial shear strength.

Keywords:

Fiber pullout, fiber-epoxy matrix, ABAQUS, Interfacial Shear Strength

1. CHAPTER ONE: BACKGROUND

1.1 Introduction

Interfacial Shear strength of fiber-epoxy interface is the main factor that determines the load transfer efficiency between fiber and matrix. Fiber reinforced composite has three components, ie. fiber, matrix and interface. A good interfacial bonding is important to the effective load transfer from matrix to fiber, which helps reducing stress concentrations In this paper the Interfacial shear strength between two natural fibers, namely Pineapple and Kapok, and epoxy is calculated and characterized. The reason to select those two fibers in combination to epoxy is because of their mechanical property, basically their elastic behavior, which is highly deviated for them to be on two extreme end points in the line of young's modulus value of natural fibers. In this paper, natural fibers are taken rather than synthetic one because of some advantages that natural fibers can bring and also natural fiber based composites are becoming favored in a way of being new emerging technology.

The method used to obtain the interfacial shear strength of Natural fiber-epoxy interface is by blending the fiber pull-out method with that of microdroplet test, the microdroplet is the epoxy that is used as a matrix. So the shape of the epoxy is spherical in order to similitude the microdroplet and the fiber which is embedded in that is pulled out in order to get the maximum force that causes the shear in the fiber-epoxy interface.

Abaqus software is used for computing the maximum force that is required to pull-out a fiber which is embedded on epoxy. Then this force, which is assumed to be cause the shear, is divided to the net contact area, which is on the interface between fiber and epoxy, to result the amount of shear strength of the interface. Different fiber diameter and length are considered in modeling. Voids are placed on the interface of some of the models in order to see study their effect on the interfacial shear strength value, which their presence on the interface resulted an increment on the IFSS value, The obtained results are discussed in comparison to interfacial shear strength values of other natural fibers from literature and also with respect to their mechanical behaviors such as elasticity, density and Poisson's ratio. The whole notion of this thesis is to study not to evaluate or compare with what is obtained by any previous experimental data.

1.1.1 Natural Fiber

Natural fibers are fibers that are produced by geological processes, or from the bodies of plants or animals. [1] They can be used as a component of composite materials.

Natural fiber may be further defined as an agglomeration of cells in which the diameter is negligible in comparison with the length. Although nature abounds in fibrous materials, especially cellulosic types such as cotton, wool, grains, and straw, only a small number can be used for textile products or other industrial purposes. Apart from economic considerations, the usefulness of fiber for commercial purposes is determined by such properties as length, strength, pliability, elasticity, abrasion resistance, absorbency, and various surface properties.

Most textile fibers are slender, flexible, and relatively strong. They are elastic in that they stretch when put under tension and then partially or completely return to their original length when the tension is removed, this figure below shows an example of natural fiber. The fibers are thin and the thickness is not uniform as shown in figure 1.

Figure 1.1 Natural fiber [2]

Natural fiber composites (NFC) are one of the most emerging natural-based products that recently have attracted more attention. As the name implies, NFC is a class of composite that contains natural fibers mixed with synthetic or bio-resins that are inherently environmentally beneficial. Other advantages of NFC are well documented in the literature, Suddel and Rosemaund [3] highlighted some advantages of NFC including low density, low cost, high toughness, acceptable specific strength properties, and excellent acoustic properties thereby reducing noise.[4]

Advantages of using natural fibers [5]

Natural fibers are popular for many different reasons, as the fabric is generally more environmentally friendly and durable.

- **Absorbent**. Natural fibers have an incredibly high absorbency, as the fibers, both plant and animal, have a strong affinity for water. This makes natural fibers a great option for bed sheets and towels, as absorbency is an important factor for these items because they're used to dry surfaces and receive regular use.
- **Eco-friendly**. Natural fibers usually have a smaller environmental impact than synthetic fibers because natural fibers do not use as many chemicals during the production process. Some natural fibers are less eco-friendly than others because some plants require more water.
- **Durable**. Due to the structure of cellulose, which makes up natural materials, most plant-based fibers are durable for frequent usage.

In addition to those main and bold advantages listed on the above section, natural fibers also have advantages such as:

- Do not produce poisonous gases when burning.
- Natural fibers are easily affordable.
- Natural fibers are safe for human skin.
- Low density
- Biodegradable

Kapok fiber

Kapok fiber is a silky cotton-like substance and originates from the Kapok tree, which is also known as ceiba kentandra. The ceiba tree belongs to the Bombacacae family and is primarily found in Asia in tropical and semi-tropical climates at an altitude less than 1000 feet, in porous volcanic soil.

Some of the characteristics of natural fibers are as follows: [18]

- Soft : gives comfort texturally
- Washable : can be washed over and over without being worn out significantly
- Buoyant : has low density than water it floats in addition of being hydrophobic
- Lofty : long strand even if the thickness is not uniform along the length
- Mold & Mildew Resistant : can resist pathogen caused mildew

Individual fibers are 0.8 to 3.2 cm (0.3 to 1.25 inches) long, averaging 1.8 cm (0.7 inch), with diameters of 30 to 36 micrometers (a micrometer is about 0.00004 inch) and has a density of 0.29g/cm3 [19].

A B

Figure 1.2: A, kapok tree and B, microscopic view of kapok fiber [20]

Pineapple fiber

Pineapple is a perennial herbaceous plant with 1-2 m for height and width belongs to the family Bromeliaceae [21]. It is chiefly cultivated in coastal and tropical regions, mainly for its fruits purpose.

Figure 1.3: Pineapple plant [22]

Natural fibers such as pineapple leaf fiber (PALF) have the advantages of low density, lightweight, low cost, biodegradability, and renewability. [79] Recently, many research works have been conducted all over the world on the utilization of natural fibers as a reinforcing material for composites for a variety of applications. The fibers from the plant can be extracted using different methods. It can be extracted using automation or traditionally by hand as shown in figure 4.

Figure 1.4: extraction of pineapple fiber from its leaf [22]

Figure 1.5: pineapple fiber [23] [24]

1.1.2 Shear strength

Shear strength is the strength of a material or component against the type of yield or structural failure when the material or component fails in shear. And Interfacial shear strength, which reflects the load transfer efficiency between the fiber and the resin, plays a significant role in determining the mechanical properties of the composite.[6]

The interface between fiber and matrix plays an important role in fiber-reinforced composite materials by affecting directly the load transfer efficiency between the fiber and the matrix as well as the mechanical properties of the composites. [7, 8] The interfacial shear strength (IFSS) is a key parameter that influences the adhesion performance between the fiber and matrix. [9, 10]

Shear strength is a material property that describes a material's resistance against a shear load before the component fails in shear. The shear action or sliding failure described by shear strength occurs parallel to the direction of the force acting on a plane. Factors such as temperature, applied load, size of the material, mechanical properties of the material will affect the shear strength of the material.

1.1.2 Failure mechanisms

In fiber-reinforced composite materials, forms of failure include fiber pullout, debonding, delamination, intralaminar matrix cracking, longitudinal matrix splitting, fiber/matrix debonding, and fiber fracture. From those fiber pullout and debonding directly deals with the interfacial contact or bonding of the fiber-epoxy matrix.

The debonding behavior of fibers strongly affects the properties of fiber-reinforced composites. A reasonable composite model needs to be consistent with a realistic description of the debonding behavior of fibers. Debonding is assumed to occur once interfacial bond strength is reached. In fracture-based approaches [12] the debonded interracial zone is regarded as a tunnel crack that grows in length once an interfacial toughness is overcome at the crack tip. There may exist a transition zone between the elastic bonded region and the frictional debonded region. The debond mode of a particular material system is determined by the size of this transition zone, in comparison to fiber-embedment length, and the difference in stress distribution between the bonded and debonded regions of the interphase. In general, a large transition zone and small difference between elastic bond strength and frictional stress will lead to a strength-controlled debond mode.[13]

Fiber pull-out is one of the failure mechanisms in fiber-reinforced composite materials. Other forms of failure include delamination, intralaminar matrix cracking, longitudinal matrix splitting, fiber/matrix debonding, and fiber fracture.[14] The cause of fiber pull-out and delamination is weak bonding.[15]

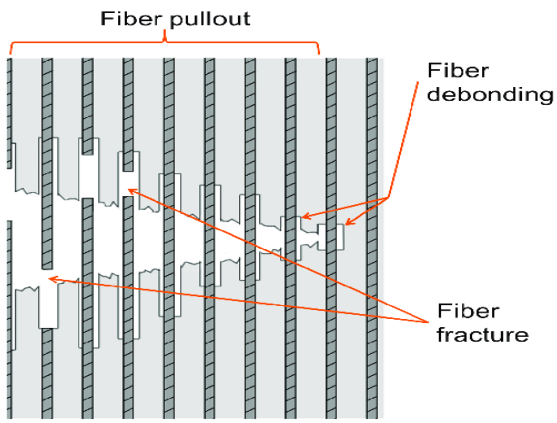

Figure 1.6: fiber failure [16]

Interfacial debonding is the detachment of fiber from the epoxy matrix, it occurs when the energy caused by tensile force surpasses the work for debonding which is calculated by:

$$W_d = \frac{\pi\, d^2 {\sigma^2}_f l_d}{24 * E_f}$$

Where:

- d is fiber diameter
- ${\sigma^2}_f$ is failure strength of the fiber
- l_d is the length of the debonded zone and
- E_f is fiber modulus

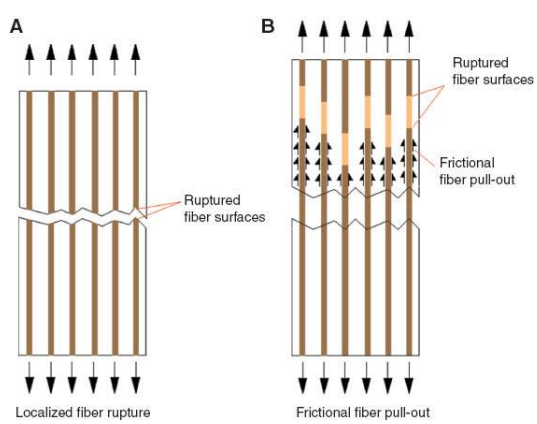

Figure 1.7: fiber-epoxy fracture failure [17]

1.2 Statement of the Problem

Natural fiber composite material is getting preferable in the emerging new technology of composite material and this domain of technology natural fiber is substituting the synthetic one because of advantages such as it has a low environmental impact, biodegradability, low density, and so on. And by not making composites to be based on natural fibers, we are losing the potential benefits that we can get from using natural fibers.

There are many composite materials that we found only synthetic fiber-based, such as grinder disk, aluminum profiles**,** etc. so if this area is researched sufficiently, we may progress to design and manufacture such products using natural fiber based on their mechanical interactive properties.

To use natural fiber as a remedy for composite material for various purposes, its mechanical property when it is embedded within a matrix has to be known. Which makes it crucial to model the interfacial shear strength of the natural fiber-epoxy matrix because interfacial shear strength is the load transfer efficiency between the fiber and the resin, which plays a significant role in determining the mechanical properties of the fiber reinforcement which is the fiber-epoxy matrix. But the interfacial strength of the natural fiber is not sufficiently studied, from the literature surveyed, upon many natural fibers, very few, i.e. bamboo's, jute, Malva fiber interfacial shear strength with matrix interface were studied.

The other gap is when IFSS of the natural-fiber epoxy matrix is studied, the presence of voids, the change in diameter and length of fiber is not considered so their effect on IFSS is unknown.

On the other hand, when a microdroplet test is performed, the process involves the use of a knife blade to push the epoxy, from fiber, which will basically damage the epoxy edge and eventually will shrink the embedded length, and also will break the fiber. In performing microdroplet test, shear blade radial distance are the most significant variable contributing to fiber breakage [80]. So there must be a means to perform a microdroplet test without damaging the epoxy or the fiber.

1.3 Significance of the study

Natural fiber-based composite is an emerging technology with minimal environmental factors. And it has a wide range of applicability. To specify the type of fiber-epoxy composition to use for materials that are needed, one must know the load transfer efficiency between the fiber and epoxy. So by studying many fibers, we can characterize the IFSS of natural fiber-epoxy matrix and this thesis is intended to study that.

Defects due to manufacturing processes such as the presence of voids or non-uniformity of the fiber, such as the change or natural variation in diameter and length of the fiber, and so on, are not considered when studying the IFSS of natural-fiber epoxy matrix and their effect on IFSS is not known. The relationship of interfacial shear strength to void, fiber length and mechanical properties of the fibers is not broadly studied in a single-fiber-epoxy matrix, so this thesis will address that.

Performing microdroplet test requires the use of a shear knife that will potentially damage the fiber as well as the epoxy, so to remove this issue; I fixed the epoxy on its outer surface, about its equator, and pull the fiber alone without damaging the edge of the epoxy neither the fiber with blades. This is a new way of blending fiber pull-out test with microdroplet test.

1.4 Hypothesis

- Natural fiber does have low tensile strength than a synthetic one; it is expected for it to fracture easily on the embedment interface between the fiber and the epoxy so that pulled out easily.
- Increasing the diameter and length size will increase the interfacial contact surface so it will make the pulling out force proportionally get increased.
- The presence of void will decrease the contact surface area between the fiber and epoxy interface and is expected to decrease interfacial shear strength of the fiber-epoxy interface proportionally.

1.5 Objectives

1.5.1 General Objective

The general objective of this thesis is to study the Interfacial Shear Strength of Natural Fibers Epoxy Matrix by Pullout Failure Mode.

1.5.2 Specific Objectives

The specific objectives of the study are:

- To determine the interfacial shear strength of both pineapple and kapok reinforced composite.
- To study the effect of change in length and diameter of the fiber and the presence of void on the interfacial shear strength of the fiber-epoxy matrix.
- To compare the IFSS result obtained to what is in the literature and conclude.
- To study the relation of IFSS and other parameters such as young's modulus and density of the fiber.

1.6 Scope and Limitations

1.6.1 Scope

This paper focuses on the failure mechanics and determining the shear strength of natural fiber epoxy interface rather than the matrix rapture or fiber breakage. The software used is ABAQUS in dynamic explicit mode. The interfacial shear strength is studied on pullout failure of the lamina and no other lamina failure because fiber pullout deals directly with the interfacial surface. The contact surface is studied under consideration as a cohesive layer.

The research did not also account in to considering environmental factors such as temperature and humidity and also the alignment of the application direction of the force that intended to pull the fiber is in parallel to the axis of the fiber along its length so no other angle is considered, the load presupposed in fiber pulling process is not cyclic or other kind but only uniform.

1.6.2 Limitations

During working this paper, there were some limitations that restrained me from progressing with momentum, from data collection to the technical mechanics of conducting the study. Some of the limitations are:

- The thesis is not inclusive of some environmental factors i.e temperature, humidity, etc. so this will possibly limit the realistic attribute or quality of the study, because it may be hard to compare with experimental result that might be done with different temperature latter on.
- During surveying and collecting the mechanical properties of natural fibers: I get different natural fibers young's modulus values from various research sites and published works so it was hard to choose one as an input value. So since the elasticity may affect the value of interfacial shear strength, having various value of young's modulus may lead one to question the reliability of the study.
- The steps of conducting numerical modeling analysis was not something available or clearly stated on previously done related works, so studying modules and watching many tutors was required which limited the thesis to propel in the desired speed.

1.7 Organization of the Thesis

The organization of the paper work of this thesis is basically in composition five chapters and each chapter discuss and contains their content as follows:

Chapter one: Background -This chapter gives an opening introduction to the reader about the research work, the problem statement, objectives, what significance this paper can bring, scopes and limitations, and how the entire thesis is organized.

Chapter two: Literature Survey- This chapter will review in detail the literature available in the area of delamination, causes, and modes of fracture, testing types to determine interfacial shear strength, and previous related works on that area.

Chapter three: Materials and Methodology – This chapter discusses the materials selected for the research, why they are selected and what are their design parameters and mechanical properties of the materials, and also the method used to conduct the thesis in finding the necessary results.: ABAQUS 3D models - this chapter is about 3D modeling and corresponding parameters of all twelve fiber-epoxy ABAQUS models.

Chapter four: Result and discussion – this chapter is about interpreting the result from ABAQUS and calculations to find IFSS. And the results are discussed and also summarizing the discussion part and giving and extrapolation of data with relation to other literature results are done in this chapter.

Chapter five: Conclusion and Recommendation – This chapter concludes the work within the relation of the objectives that are presupposed for the research.

2. CHAPTER TWO: LITERATURE REVIEW

Studying the interfacial shear strength of the natural fiber-epoxy composite is necessary since it determines the load transfer efficiency of the composite. In the case of natural fibers, this area is studied barely.

In this literature survey, different failure mechanisms and failure modes that can happen in composite materials are surveyed. A previously works in studying the IFSS of the fiber-epoxy interface using different techniques are also surveyed. And some gaps are identified as a problem that seeks to be filled and improved.

2.1 Interfacial Shear Strength

The interfacial strength refers to the strength of the bond between the matrix phase and the dispersed phase. Usually, interfacial strength is desired. [25]
Interfacial shear failure on the interfacial surface of fiber – epoxy matrix due to fiber pull-out is a mode II crack.

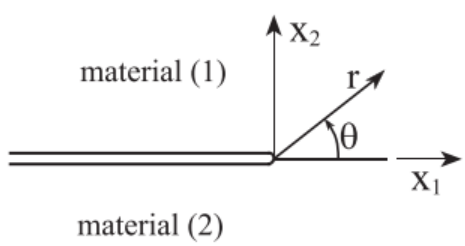

Figure 2.1 Interface crack tip geometry [26]

The composite interfacial shear strength, which reflects the load transfer efficiency between the fiber and the resin, plays a significant role in determining the mechanical properties of the composite [27].

The fiber-matrix interfacial shear strength is the main factor determining the mechanical properties of composite materials. [28] The magnitude of the interfacial shear strength is based on the surface properties of both components [29].

2.2 Delamination

Delamination is a common failure mode in composites. It often leads to structural disintegration before fiber failure, thereby compromising the overall load-carrying capability of composite structures. While different methods exist to model delamination, arguably the most widely used ones are based on cohesive elements (CEs). The CE is an interface element established based on the cohesive zone model. [30]

Delamination is a failure in laminated material, often a composite, which leads to the separation of the layers of reinforcement or plies. Delamination failure can be of several types, such as: [31]

- fracture within the adhesive or resin
- fracture within the reinforcement
- debonding of the resin from the reinforcement

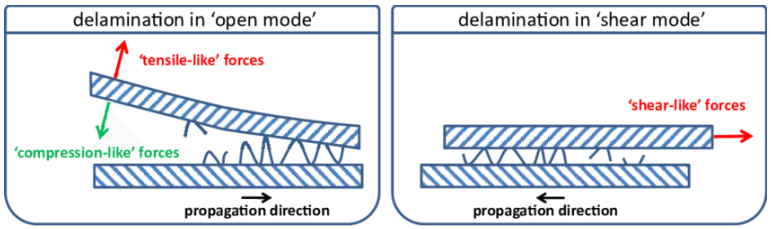

Figure 2.2 Delamination modes [32]

Delamination is caused when a laminated material becomes separated; perhaps induced by poor processing during production, impact in service, or some other means.

2.2.1 Some Causes of delamination

Delamination can occur in various different ways, the main reasons why delamination is occurred by is because of the formation of: [33]

- Matrix cracking
- Bending cracks, and
- Shear cracks.

2.2.1.1 Matrix cracking

Matrix cracking is a Major pattern of the failure of composite materials. A crack can form in the matrix during manufacturing, or be produced during loading. [34]

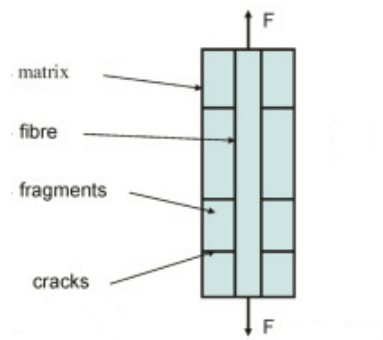

Figure 2.3 Typical matrix cracking [35]

2.2.1.2 Bending cracks

Bending cracks/Flexural cracks on the sides of a beam starts at the tension face and **will extend**, at most, up to the neutral axis. In general, the cracks will be uniformly spaced along the most heavily loaded portion of the beam, i.e. near the mid-span in sagging or over the supports in hogging. [36]

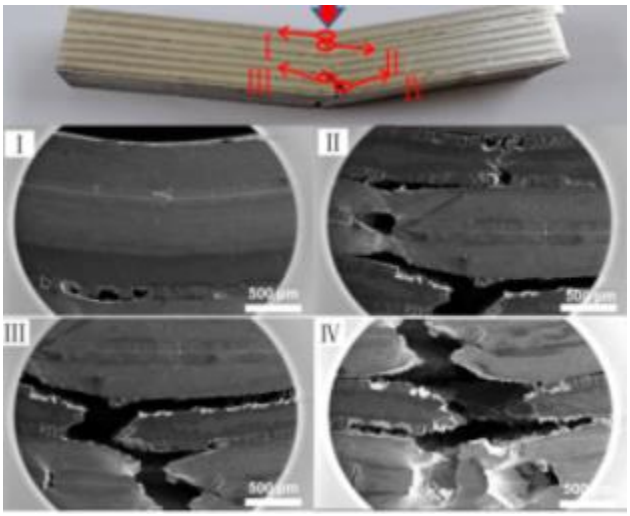

Figure 2.4 the macro morphology of AlMgTi-based composite bending crack. [37]

2.2.1.3 Shear cracks

Shear cracks are developed when the acting shear on the section exceeds the resisting shear capacity in certain situations it is likely that a particular structural member will show the formation of shear cracks over its surface and it is valid to any member which encounters shear.

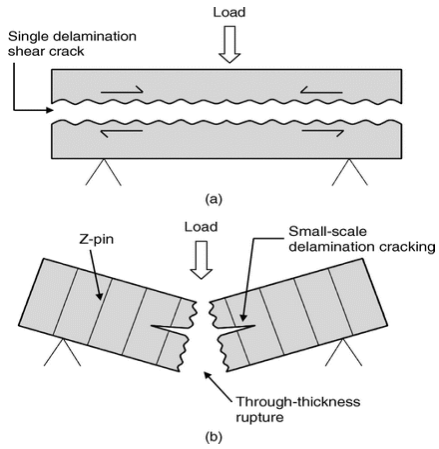

Figure 2.5 Typical Shear crack across the length and through-thickness [38]

2.3 Fracture Mechanics

2.3.1 Loading Modes

In general, an object can be loaded in any direction relative to the crack. The sketch at the right shows a force vector at such a random orientation. It is mostly perpendicular to the crack, but also contains components that produce in-plane and out-of-plane shear.

When this occurs, the logical thing to do is partition the force into its fundamental components. This process leads to the three loading modes shown in figure 2.6.

Mode I Loading occurs the most often and produces the most damage. Because of this, it naturally receives the most attention in research, structural design, failure analysis, etc. It is commonly called the *Opening Mode*.

Mode II Corresponds to shearing of the crack face due to in-plane shear stresses. It probably receives the second most attention because the problem is still 2-D since all the action is *in-plane*. Mode II loading influences crack growth direction in a way that minimizes further Mode II loading while maximizing Mode I.

Mode III It is the *Tearing Mode* for obvious reasons. It is driven by out-of-plane shear stresses and does not seem to occur as often as the other two. [39]

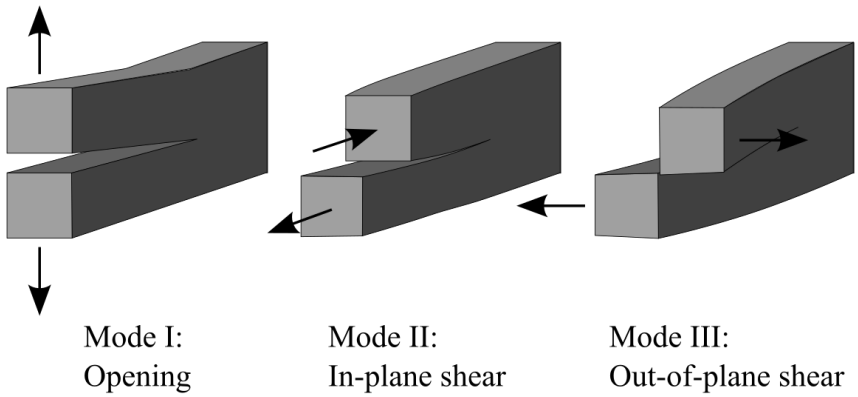

Figure 2.6: Loading modes [39]

2.3.2 Shear fracture Mode II

Mode II is also known as sliding mode and occurs when shear stress is applied parallel to the plane of the crack and perpendicular to the crack front [40].

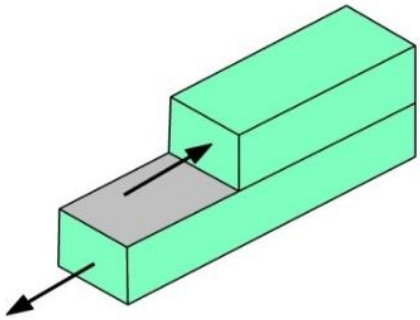

Figure 2.7: Typical mode II in-plane shear fracture [82]

2.4 Cohesive layer

The cohesive layer methodology has proven to be a powerful tool for the study of delamination growth in laminated composites. It is based on the postulation of a layer of cohesive material between the surfaces liable to delaminate and an energy release criterion for its decohesion. A Majority of the investigators have used cohesive layers of zero thickness; although there is an implicit recognition of a cohesive zone upstream of the crack tip which must necessarily have some thickness, however small. The cohesive law takes the form of a relationship between the relative displacements between the delaminating layers and the interlaminar stresses. [41]

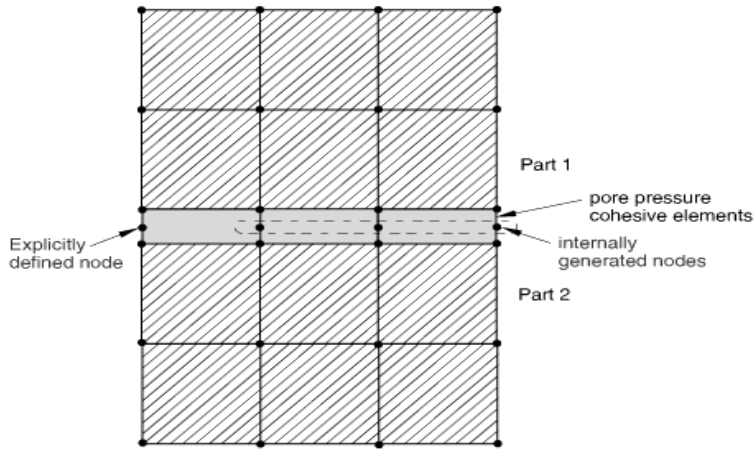

Figure 2.8: Cohesive elements sharing nodes with other Abaqus elements [42]

2.4.1 Cohesive Zone Mode

The cohesive zone model implies that normal stress continues to be transferred across a discontinuity which may or may not be visible as shown in Figure 16.

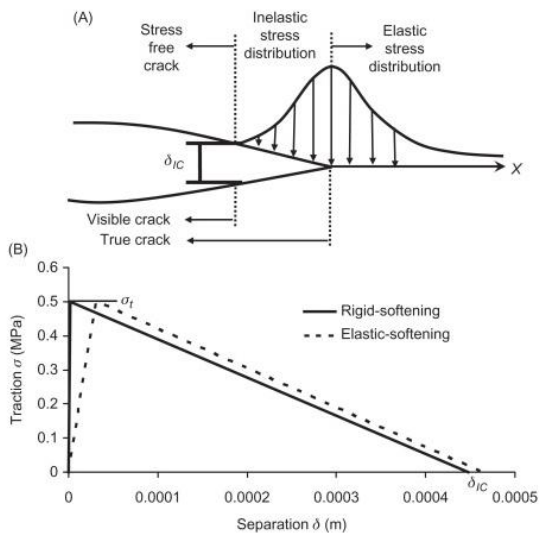

Figure 2.9: Representation of the fracture process zone & the constitutive cohesive zone [43]

2.5 Testing Interfacial shear strength

The micromechanical techniques available for the measurement of single fiber interfacial shear strength include a fragmentation test (Godara et al., 2010), single fiber pull-out (Nova et al., 2013), single fiber push-out test (Sharma et al., 2012), and microdroplet test (Kang et al., 2009). [44]

2.5.1 IFSS Testing method types [49]

There are various ways by which we can conduct a processes or steps to determine an interfacial shear strength value of composite.

The main four Interfacial Shear Strength testing types are:

- Fragmentation test
- Single fiber pull-out
- Fiber push-out test
- Microdroplet test | progressive debonding

2.5.1.1 Fiber fragmentation test

The fragmentation test is developed from the early work of Kelly and Tyson [87], who investigated brittle tungsten fibers that broke into multiple segments in a copper matrix composite. Each test specimen for the fragmentation test consists of one fiber encapsulated in a chosen polymer matrix. The specimen normally has a dogbone shape. Elongating the specimens in a tensile tester results in fiber breakage. This experiment is done under a light microscope so that the fragmentation process can be observed in-situ. The fiber inside the resin breaks into increasingly smaller fragments at locations where the fiber's axial stress reaches its tensile strength. This requires a resin system with a sufficiently higher strain-to-failure than the fiber's. When the fiber breaks, the tensile stress at the fracture location reduces to zero.

Due to the constant shear in the matrix, the tensile stress in the fiber increases roughly linearly from its ends to a plateau in longer fragments. The higher the axial strain, the more fractures will be caused in the fiber, but at some level the number of fragments will become constant as the fragment length is too short to transfer enough stresses into the fiber to cause further breakage.

The fiber fragmentation test is again a single-fiber micromechanical test in which the single fiber embedded in a dog bone-shaped matrix is pulled under tension until equilibrium with multiple fragmentations of the fiber occurs. [45]

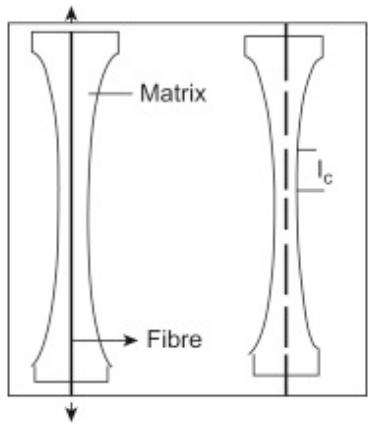

Figure 2.10: Fiber fragmentation [45]

The interfacial shear strength τ_i is given by a consideratio of the stress transfer between the fiber and matrix. [46]

$$\tau_i = \frac{d_f \sigma_{fu(l_c)}}{2l_c} \tag{2.1}$$

Where:

l_c = the equilibrium critical length of the fiber

d_f = the fiber diameter, and

$\sigma_{fu(l_c)}$ = the fiber strength.

Single fibre fragmentation tests are performed for brittle fibres with Weibull strength distribution and different surface treatments. The fragmentation process is modelled and closed-form expressions for break spacing distribution. Fragment length distribution is predicted for several load levels. [90]

2.5.1.2 Single fiber pull-out

Single-fiber pullout testing is a well-documented method that allows for the measurement of the debonding load between the matrix and embedded fiber [47].

Fiber pull-out is one of the failure mechanisms in fiber-reinforced composite materials.[47] Other forms of failure include delamination, intralaminar matrix cracking, longitudinal matrix splitting, fiber/matrix debonding, and fiber fracture.[47] The cause of fiber pull-out and delamination is weak bonding.[48]

Work for debonding is given by [49]:

$$W_d = \frac{\pi d^2 \sigma^2{}_f l_d}{24 E_f} \tag{2.2}$$

Where:

W_d = work for debonding

d = fiber diameter

$\sigma^2{}_f$ = failure strength of the fiber

l_d = length of the debonded zone

E_f = fiber modulus

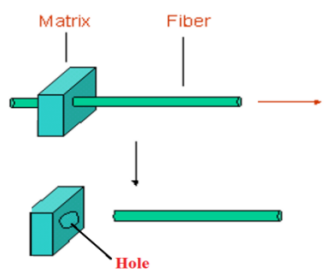

Figure 2.11: pulling out a single fiber from matrix [50]

From the study by Surendra P. Shah and Yeou-Shang Jenq on Fracture Mechanics of Interfaces Interfacial bond properties between fibers and matrix are investigated. A fiber pull-out test, which is commonly used to study the interfacial bond strength of the fiber-matrix system, is analyzed. The bonding between fibers and matrix are assumed to be perfect before the pull-out load is applied. Griffith energy criterion is used to govern the crack propagation at the interfacial region when debonding Constant frictional shear stress, which may be a result of the existence of surface roughness at the interface, is assumed to exist at the wake of debonding region. Based on this mechanism, the total pull-out load can be decomposed as the resistance offered by the interfacial bond and resistance offered by the frictional stress. The proposed approach is applicable to any elastic fiber and matrix system, but only the results of steel fibers and reinforcing bars in a cementitious matrix are reported. The proposed model correctly predicts several experimental trends of bond strengths reported by other researchers. Furthermore, theoretical predictions of progressive failure of bond cracks are found to be in good agreement with a holographic interferometry study on a pull-out test. [57]

The research was done on the Interfacial Characterization by Pull-Out Test of Bamboo Fibers Embedded in Poly (Lactic Acid); shows the apparent shear strength at the interface between bamboo fiber and the surrounding poly (lactic acid) (PLA) matrix is quantified. A method for processing pull-out test samples within a controlled embedded length is proposed and the details of the test procedure are presented, along with a critical discussion of the results.

Two series of samples are considered: untreated and mercerized bamboo fibers from the same batch, embedded in the same polyester matrix. Electron and optical microscopy are used to observe the fiber-matrix interface before and after the test, and to identify the failure mode of each sample, especially as regards the occurrence of fibrillation in the fiber bundles. The values of apparent interfacial shear strength are calculated only for regular fibers successfully pulled out from the matrix, and reported with their statistical variations.

Mercerization, whose efficiency was proven by Fourier transform infrared (FTIR) spectroscopy, did not appear though to improve the quality of the interface ($\tau app = 7.0 \pm 3.1$ MPa for untreated fibers and $\tau app = 5.3 \pm 2.4$ MPa for treated fibers). [58]
The diameter of the fiber used in this experiment varied from 55 ± 3 mm. The IFSS was found to be 4.91 MPa for the bamboo fiber/PP system. The IFSS value was found to be 2.14MPa for the jute fiber/ PP system. The IFSS value of bamboo fiber/PP composite was higher compared to the jute fiber/PP composite. [59]

The most *common* way to observe the interface effect is through *fiber pullout tests,* which consists of debonding process and followed fiber *pullout* process. [60]

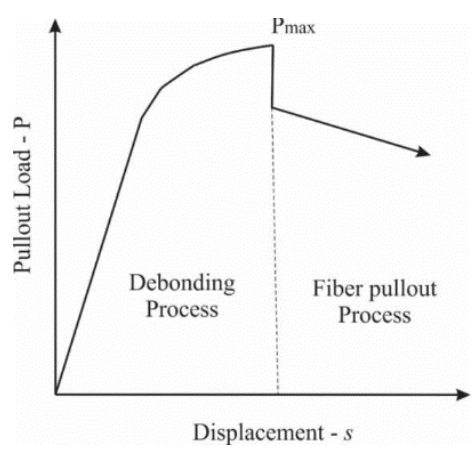

Figure 2.12: Typical fiber pullout test curve. [61]

The other numerical analysis of pull out test that I got is on the pull out of rod from concrete theoretically, that is relatable, and here is the paper's abstract:

The computational and simulation analysis of pull-out fiber reinforced concrete was investigated. The finite element analysis was used to make this modeling and analysis on this reinforced system and three parts (concrete matrix, the placed fiber reinforcement polymers (FRP), and resin layer) were studied. A constant load was directly applied on the free end of placed FRP and the deformation, von Mises stress, displacement, and strain of these three analyzed parts were obtained. Meanwhile, the specimen system of bonding strength and strain was calculated by the method of ABAQUS. The results showed that, with the constant load, the von Mises stress, deformation, and strain appeared in these three parts, and the maximum values in both FRP and resin layer were shown at the free end side, which provides an accurate description of the rupture mode.[62]

2.5.1.3 Fiber push-out test

The fiber push-out test is a mechanical test performed on composite materials where fiber is mechanically pushed out of the material. This test is carried out with the purpose of measuring the matrix/fiber interface de-bonding energy and the effects of frictional sliding between the matrix and the fiber. [52]

The mechanics behind the test are as follows: [88]

1. Elastic loading: the flat tip indenter is lowered onto the fiber using a CCD camera to guide the indenter downwards
2. Progressive de-bonding: the indenter touches the fiber and begins applying load, bonds begin to break between the matrix and the fiber
3. Fiber push through: the bonds between the matrix and fiber are totally broken and the fiber begins to slide out of the matrix
4. Interfacial sliding: the indenter continues to push the fiber through the matrix, the only force resisting this movement is frictional
5. Indenter matrix collision: the fiber has been totally pushed out of the matrix and the indenter collides with the matrix surface. This gives the total displacement of the fiber.

A 2016 study on comparison of fiber push-out and fiber pull-out test for measuring interfacial shear strength in nano-reinforced composite materials shows that on the influence of the carbon nanotubes (CNTs) content on the fiber/matrix interfacial shear strength (IFSS) in glass/fiber epoxy composites was measured by means of push-in and push-out tests shows that both experimental methodologies provided equivalent values of the IFSS for each material. [89]

2.5.1.4 Microdroplet test

The microdroplet technique is usually designed as a fiber embedded in a drop of resin and subsequently pulled out while the drop is being supported by two knife edges, resulting in either debonding of the droplets from the fibers or breakage of fibers before debonding can occur. [51]

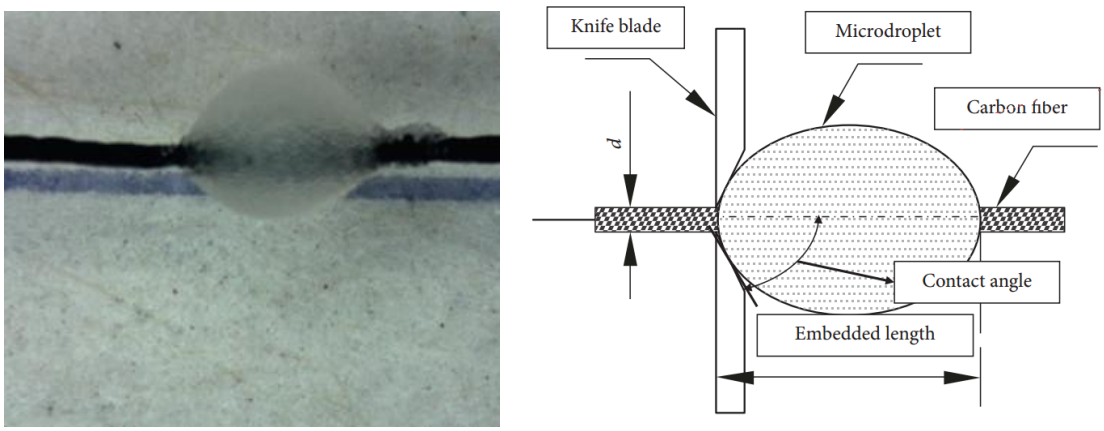

A B

Figure 2.13: Fiber in epoxy microdroplet A [27], Microdroplet test B [53]

So by modeling this microdroplet technique through ABAQUS and applying force through the knife, we will measure how much the fiber displaced. So finally force to displacement graph will be presented to characteristics of the interfacial shear strength of the fiber-epoxy matrix.

The required force to pull out the fiber of cured epoxy resin is measured for each specimen and the interfacial shear strength τ_{IFSS} was estimated by: [54]

$$\tau_{IFSS} = \frac{F_{max}}{\pi . d_f . l_e} \tag{2.3}$$

Where:

F_{max} = the maximum value of pull-out force.

d_f = the diameter of a single fiber.

l_e = the embedded length of a fiber in the microdroplet.

The failure model of traction-separation used in this study is quadratic stress failure criterion [55] and a Benzeggagh-Kenane (BK) criterion [56] to evaluate, respectively, both the initial damage and crack propagation.

The quadratic stress failure criterion was expressed through.

$$\left(\frac{max\langle\sigma_n, 0\rangle^2}{N_{max}}\right) + \left(\frac{\sigma_t}{T_{max}}\right)^2 + \left(\frac{\sigma_s}{S_{max}}\right)^2 = 1 \qquad (2.4)$$

Where:

σ_n, σ_t and σ_s and are the stress components of pure normal direction, first shear direction, and second shear direction.

N_{max}, T_{max}, and S_{max} are the interfacial strengths of pure normal direction, first shear direction, and second shear direction.

2.5.2 INFSS test using microdroplet test

The microdroplet test is one of the most widely adopted micromechanical tests to characterize the interfacial properties between resin matrix and single filaments. [64] [65]

The microdroplet technique is usually designed as a fiber embedded in a drop of resin and subsequently pulled out while the drop is being supported by two knife edges, resulting in either debonding of the droplets from the fibers, or breakage of the fibers before debonding can occur.[60] A study on experimental and finite element analysis of the dependence of failure mode on droplet shaped Composite Interfaces by Hodzic, A., Kalyanasundaram, S., Lowe, A., & Stachurski, Z. H, which the microdroplet technique was performed using a platinum ring with a 40 μm hole instead of the usual two knife edges, giving an axisymmetric geometry, load and stress distribution. Glass/phenolic and glass/polyester composite systems were tested experimentally and subsequent finite element modeling studies were performed to assess the variation of droplet size, and contact angle between the droplet and fiber. It was found that contact angle is of Major influence in the proposed failure model. The study characterizes the influence of the contact angle between the droplet and the fiber on the subsequent stress distribution in the microdroplet specimen. [60]

In the research done by the title of “Finite element study of the microdroplet test for interfacial shear strength: Effects of geometric parameters for a carbon fiber/epoxy system”. A 3D finite element model has been developed to identify the main causes of variability in the microdroplet test, which is commonly used to characterize the interfacial shear strength between polymer matrices and single filaments. A more realistic droplet shape and test configuration, including meniscus details and prismatic shear blades, have been modeled for a carbon fiber/epoxy system to simulate a more representative setup than is commonly used in the literature.

The interfacial behavior has been modeled using a cohesive surface contact and fiber breakage has been captured using a maximum stress criterion. A statistical study has been performed to systematically evaluate the influence of key geometrical test parameters on the variability in the measured interfacial shear strength values and the likelihood of fiber breakage. Parameters studied are fiber embedded length, fiber diameter, shear blade radial opening distance, and shear blade axial misalignment.

Results of the studied carbon fiber/epoxy system suggest that fiber embedded length and the combined effects of the shear blade radial distance and the shear blade axial misalignment are the most significant sources of variability for the measured interfacial shear strength. However, fiber embedded length and the shear blade radial distance are the most significant variables contributing to fiber breakage. [66]

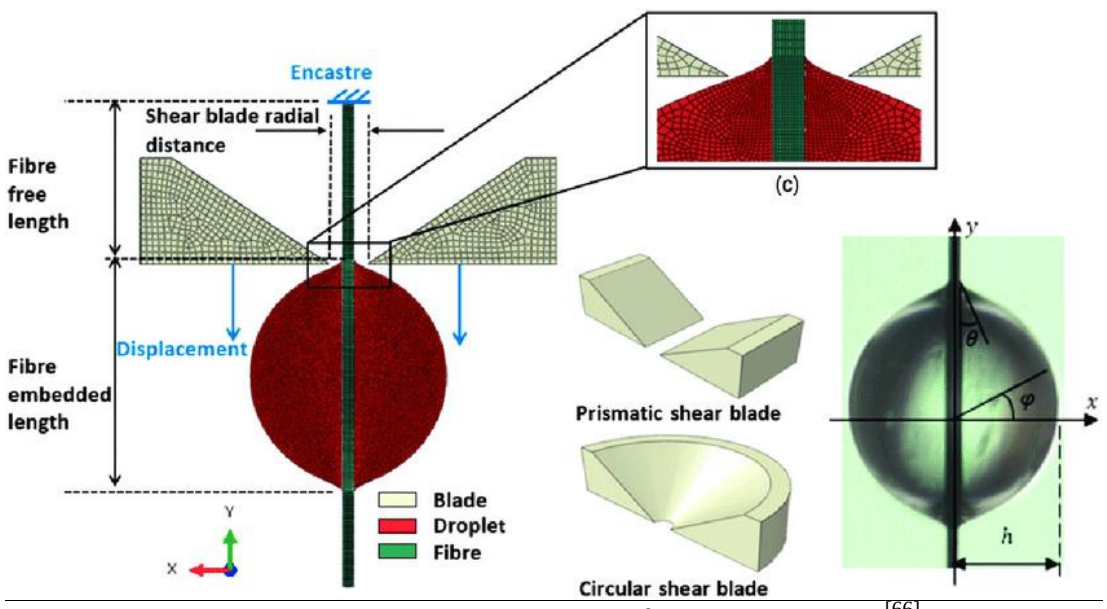

Figure 2.14: Numerical modeling of microdroplet test [66]

2.6 Voids in composite material

Voids, the most studied type of manufacturing defects, form very often in the processing of fiber-reinforced composites. [67] Voids in fiber-reinforced composite materials are areas that are absent of the composite components: matrix (resin) and fibers. Voids have many causes but generally can be categorized as voids due to volatiles or as voids that result from entrapped air.

A void is a pore that remains unfilled with polymer and fibers in a composite material. Voids can act as crack initiation sites as well as allow moisture to penetrate the composite and contribute to the anisotropy of the composite. [60]

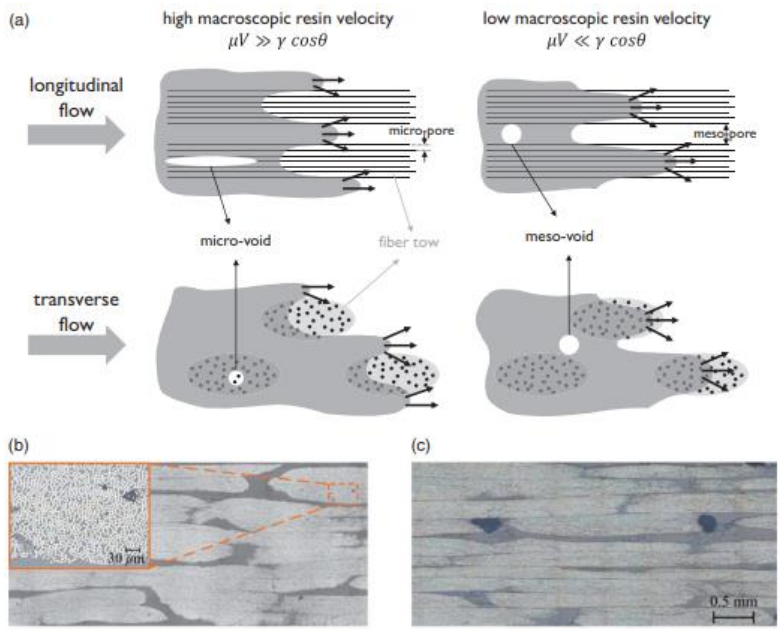

Figure 2.15: (a) Schematic of void formation during longitudinal and transverse flow in the liquid composite molding of a dual-scale fibrous preform (b) micro-and (c) meso-voids inside and between tows, respectively [69]

From a study by Chengdu Aircraft Industry on the void, the analysis results show that compaction pressure during the manufacturing process influences the porosity of laminate area. Increasing the compaction pressure and compaction time will reduce the porosity of the laminates. [69]

There is no data regarding to the percentile volume or distribution of voids on the interface of single fiber-epoxy matrix.

2.7 Summary of the literature and Identified gaps

From observation in the study of the literature; the interfacial shear strength of natural fiber-epoxy matrix is barely studied and those studies do not consider the defects that can happen in the production composite such as the presence of void and the inconsistency of the diameter of natural fibers when extracted which is the non-uniformity of fibers in diameter and length.
From many commercially available natural fibers with different mechanical properties, the only fibers that are used in order to study IFSS of their interface with epoxy are Bamboo and Jute. So the area is not well studied.

The other gap is, even though the microdroplet test is considered to be the most effective widely used technique to study the interfacial shear strength, it has its own drawback as a study by Zhao, Q., Qian, C. C., Harper, L. T., & Warrior, N. A. (2018). Titled "Finite element study of the microdroplet test for interfacial shear strength: Effects of geometric parameters for a carbon fiber/epoxy system." Showed, when modeling microdroplet test through FEM, the shear knife that used to push the epoxy to delaminate if from the fiber embedment will potentially cause damage to the fiber and epoxy. So in the numerical realm, the involvement of a knife is not necessary since we can directly apply a force to pull the fiber out from its epoxy embedment with our using a shear knife as an agent of means to push.

When pulling out fiber from its epoxy embedment is subjected to shear fracture. And the type of failure which will be caused on the interface is mode II shear failure. This thesis is basically focused on that. The basic 3D model used in this thesis is to pull the fiber out from a microdroplet of epoxy and this can be shown as it is sketched in figure 23.

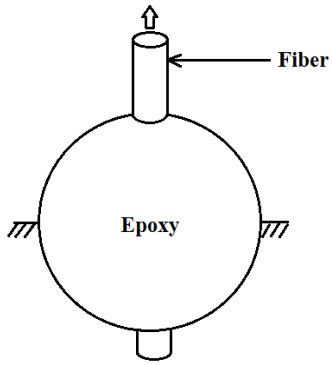

Figure 2.16: A typical sketch of the fiber-epoxy model that is used in this thesis

From the type of shear failure; the failure approach in this research, which is pulling of out fiber from its epoxy embedment, is mode II shear failure because the failure in the interface is an in-plane shear failure and also the force that will cause the interface to fracture is applied in the direction which is parallel to the shear plane. And the interfacial shear strength value is calculated using the formula [54].

$$\tau_{IFSS} = \frac{F_{max}}{\pi . d_f . l_e} \tag{2.3}$$

Where:

F_{max} = the maximum value of pull-out force.

d_f = the diameter of a single fiber.

l_e = the embedded length of the fiber in the microdroplet.

3. CHAPTER THREE: RESEARCH METHODS AND MATERIALS

3.1 Materials

By considering the mechanical properties of natural fiber [3] two natural fibers are chosen.

By taking fibers with highest and lowest young's modulus value among natural fibers, the chosen fibers are:

- **Pineapple fiber** which has high young's modulus value and
- **Kapok fiber**

Those two fibers are chosen based on their mechanical properties since pineapple fiber has the highest tensile strength and highest young's modulus and kapok has low tensile strength and lowest young's modulus among natural fibers. [3] Those two natural fibers having this different strength range are selected in supplication to reflect the rare end opposite mechanical property values of natural fiber and to characterize IFSS based on it. The IFSS of two fibers having medium elasticity has already been studied. So it will be good to take those fibers and to contrast the result.

The two fibers are used in combination of

- **Epoxy with resin** as the matrix.
- **Cohesive layer** on the surface of the matrix wshich is in contact with the fiber.

3.1.1 Dimensions and other parameters

Usually, the diameter of kapok fiber occurs with diameters of 30 to 36 micrometers [70]. And the density of kapok fiber is 0.29 g/cm^3. [27] There is no data that tells the Poisson's ratio of kapok fiber so the Poisson's ratio of kapok fiber from its bulk modulus is calculated as such:

Bulk Modulus is given by: [22]

$$K = \frac{E}{3(1-2v)} \tag{3.1}$$

From this; Poisson's ratio v is:

$$1 - 2v = \frac{E}{3K} \tag{3.2}$$

$$v = -\left(\frac{\frac{E}{3K} - 1}{2}\right) \tag{3.3}$$

$$v = \frac{1}{2} - \frac{E}{6K} \tag{3.4}$$

Bulk modulus value for kapok is $2.93 * 10^5\ psi$ [78] which is around$\simeq 2.02\ GPa$, and it's Young's Modulus is 4 GPa. So by substituting those values on equation 3.4, we get:

$$v = \frac{1}{2} - \frac{4}{6 * 2.02}$$

$$v_{Kapok} = 0.17$$

The diameter of a single pineapple fiber is 48 micrometers [31] considering the possibility of the existence of a defect in fiber and since fiber cannot be found in uniform size naturally, I took 45 to 51 micrometers. Its density is 1.07 g/cm^3 [26] and has a Poisson ratio of 0.35 [21].

The diameter of the epoxy droplet is dependent on the embodied fiber length, its young's modulus is 4.6 GPa [24] and its density is 1.12 g/cm^3 [28], and has a Poisson's ratio of 0.389 [25].

Table 1: Design parameters

	Diameter (μm)			**Embedded Length (mm)**		**Young's Modulus (GPa)**	**Density (g/cm^3)**	**Poisson's Ratio**
	Min	Max	Avg.	Min	Max			
Pineapple	45	51	48	0.1	3	71	1.07	0.35
Kapok	30	36	33	0.1	1	4	0.29 [84]	0.17
Epoxy	Sphere Ø is according to the EL of the fibers					4.6 [24]	1.12 [28]	0.389 [25]

The interface is subjected to a coefficient of friction of 0.58 for most natural fibers [72] in addition there I form a cohesive layer between the matrix and fiber, which is the inner face of the epoxy, and is with zero thickness but a very small (one tenth of the material thickness) out of surface thickness is taken, so the property will become defused to the parts within that extent of range without the surface physically appeared.

So there will be a smooth translation of material property in the interface boundary between the fiber and epoxy.

Table 2: Parameter of cohesive zone

	Cohesive Zone Mode	
Mechanical properties and parameters	Young's Modulus in GPa	4.6
	Coefficient of friction	0.58
	Tensile strength in MPa	25 [62]
	Thickness	0

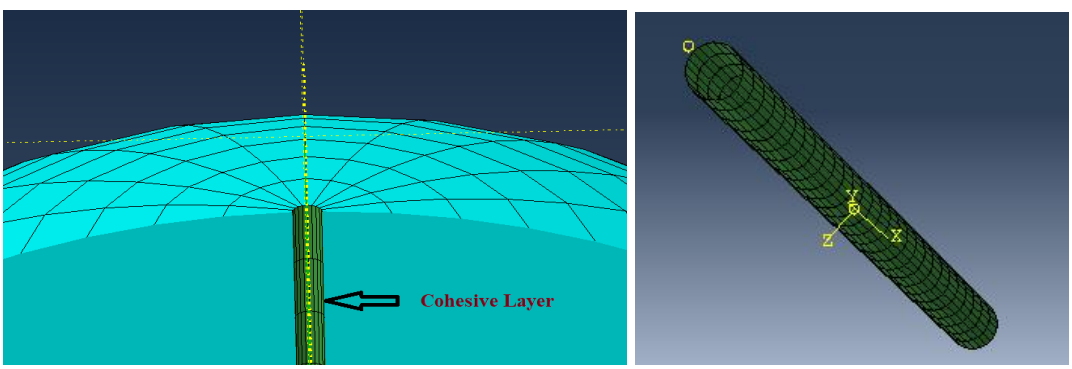

A B

Figure 3.1: Sectional view of epoxy with cohesive layer (A) and cohesive layer in 3D (B)

3.2 Method and steps

3.2.1 Method

The research is conducted using a combination of pull out and microdroplet test. Meanwhile in order to remove the problem of conducting microdroplet test through software, the problem which is cause by the involvement of shear blade, by only taking the shape of the microdroplet and instead of using shear blade the fiber is pulled-out from its' epoxy embedment which will makes the stem a combination of microdroplet and fiber pull-out test.

From the four IFSS tests, the fiber pullout test is a common preferable IFSS test [60] microdroplet test is usually used for experimental propose, in the numerical world there is no need for a knife to push the epoxy, the knife distorts the epoxy or because of the elastic property of the epoxy, the epoxy dumps some of the force, which is applied on the knife, before it gets distributed and moves the epoxy at the whole, which can be considered as a drawback, so in order to minimize the force is directly applied on the fiber since it is possible in the numerical realm.

Thus the middle outer edge of the epoxy is fixed and the fiber is pulled out from the epoxy matrix. This makes the method as a pulling fiber out of microdroplet of epoxy matrix.

The steps that are used as a method in this paper are:

- Modeling the parts within specified parameters and the assembling.
- Inputting mechanical properties of the materials in property assigning part of abacus.
- Then, define the interaction type which is cohesive zone mode by inserting z cohesive layer in between the contact surface of fiber epoxy.
- Then defining the boundary conditions:
- Defining reference point along the axis in the direction of the length of fiber on which the pulling force ought to be exerted.
- Giving how a value of long should the fiber has to be pulled out in the direction of the axis ere the reference point is aligned up.
- And finally, get the amount of force needed in the process of pulling out the fiber from the epoxy matrix.
- The finally analytically calculating the interfacial shear strength and correlate with parameters to find some relation.
- Compare to some interfacial shear strength values got in the literature then finally make correlation and conclude.

3.2.1.1 Software used

Since the thesis is mainly based on the result for the numerical analysis so the outcome results are highly dependent on the software capability and features, it was needed to choose upon different software available to compute fiber-epoxy interface shear.

Some of commercially available software:

- ABAQUS
- Altair HyperWorks
- Ansys LS-DYNA.
- Fusion 360
- Inventor
- MATLAB
- COMSOL Multiphysics (formerly FEMLAB)
- Ansys Mechanical etc.

From those commercially available software, ABAQUS is selected because of:

- Availability
- Able to compute with explicit and implicit modeling options
- Almost all computing regarding fiber-epoxy interface are done using this software
- Can be accessed easily not costly
- Many tutorials and manuals can be accessed
- Easy to use and model on it

Dynamic Implicit is a type of analysis in which static, the time incrimination is big. It is very slow that the effect of inertia on the loading process is negligible. It is so slow to the degree that the analysis is considered static. In Dynamic Implicit there is no effect of inertia on the loading because the loading is extremely low, the density of the material has no effect on the result of the analysis. It also inverts the stiffness matrix to perform iteration. This method requires additional computation and can be harder to implement. However, it will be used in lieu of explicit methodologies when problems are still and using alternative analysis methods is impractical. The implicit method should be used when the events are much slower and the effects of strain rates are minimal. Once the growth of stress as a function of strain can be established, these can be analyzed using implicit methods. In this case, one can consider a static equilibrium such that: Sum of all forces = 0

But in the case of **Dynamic Explicit**, which is a quasi-static analysis that means there is an inertia effect on the loading; the time increment is small and is so the whole process is relatively fast. Changing the density can change the inertia so will influence the result too. Explicit FEM is used to calculate the state of a given system at a different time from the current time. In contrast, an implicit analysis finds a solution by solving an equation that includes both the current and later states of the given system. Explicit analysis offers a faster solution in events where there is a dynamic equilibrium or otherwise: Sum of all forces = mass x acceleration

3.2.2 ABAQUS Steps

Most of the numerical analyses of fiber epoxy are done using ABAQUS software. In pulling the fiber out of its epoxy matrix embedment, the Major steps/flow if modeling fiber-epoxy interface is as such:

Create Model
↓
Material property → assign material property
↓
Create step
↓
Create reference point
↓
Create interaction → Tangential interaction
→ Cohesive interaction
↓
Create boundary condition → Condition 1 - displacement
→ Condition 2 - boundary fixing
↓
Mesh
↓
Job
↓
Interpretation ← Result

Using ABAQUS 2020 version the steps are as follows:

Create model: by opening the database with standard/explicit mode. Model the fiber epoxy using the steps as follows:

1. by selecting a part from options under module, select "create part"
2. select the modeling space to be 3D
3. enter the name whether it is fiber or epoxy then enter the dimensions of the models accordingly

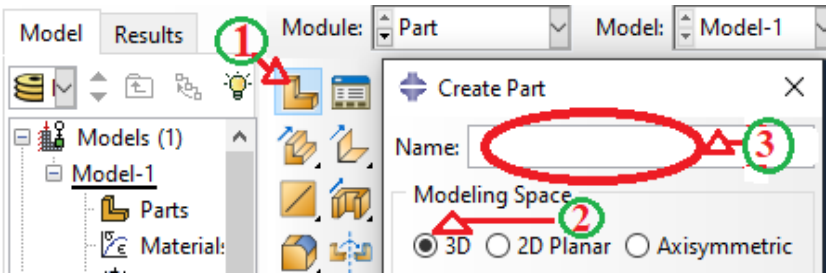

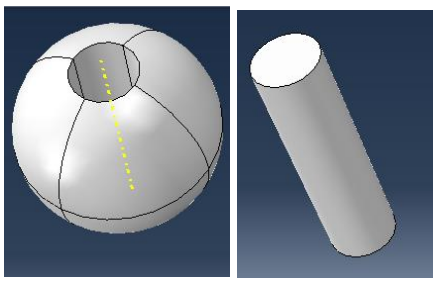

Create material properties in this step, the material property is created based on the mechanical property that fibers and epoxy possessed

1. select “Property” from Module and the properties “create material”
2. give a name for the set of properties (which latter be assigned)
   Under material behaviors bar:
3. select “Elastic” from material behavior under “Mechanical”
4. select “Isotropic” from “type” (since epoxy and each fiber are isotropic independently”
5. give young’s modulus and poison’s ratio value accordingly

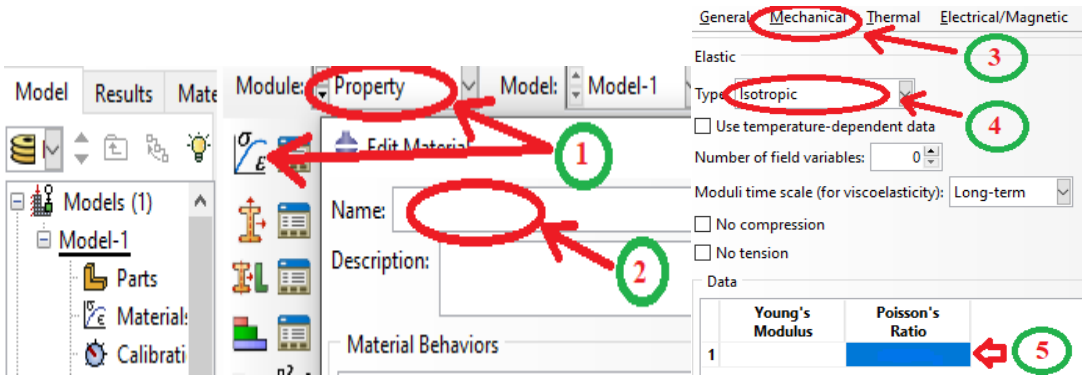

Assign material properties | here in order to assign the material property for each created 3d models we have to go under some steps as follows:

1. from the module select “property”
2. select “Edit assign section”

   Then by using curser, select the 3d model and click done
3. then select “create section”

   When selecting “create section”, a new window will pop out
4. then since both solidified epoxy and fiber are homogeneous
5. select "Homogeneous" from solid type under category
6. give a name for the section selected then click ok
7. From a new window opened, select a downward cursor symbol to select among material properties (which are previously created), then select ok.

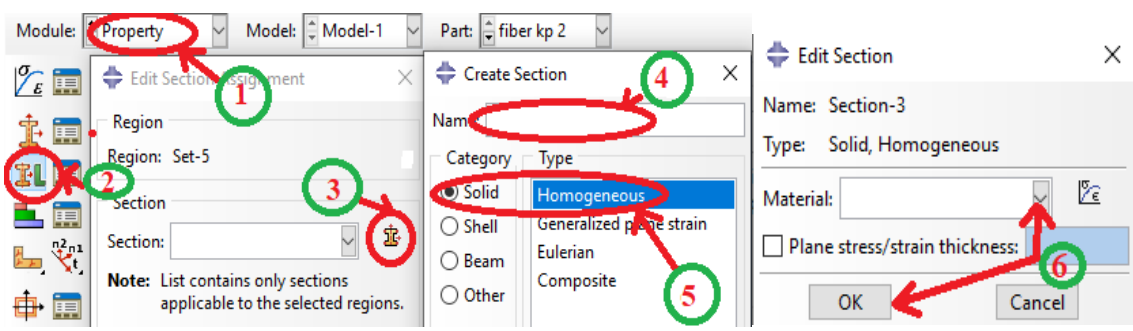

Create cohesive surface: The reason why the interface is selected to be cohesive is because of by considering the concept which is since natural fibers are spongy so that the epoxy will penetrate the fiber to some depth so that the fiber will attain neo epoxy property on it’s our surface so that the bond in the interface will be cohesive.

This step is to show how cohesive element is created on the fiber-epoxy interface.

1. Select "mesh" from the module and click on the mesh from the toolbar
2. Select “Edit”
3. Select "mesh" from the category and then select "offset" to create a solid layer
4. Select the element face to be “by angle”
5. Select the face which we want it to be cohesive, in our case It is the inside surface of the epoxy on which the fiber is ought to be embedded, and then click on "done"
6. Since we don’t want additional extruded thickness but only a surface with cohesive property, make the thickness 0
7. Give a name for the layer then click on "ok"

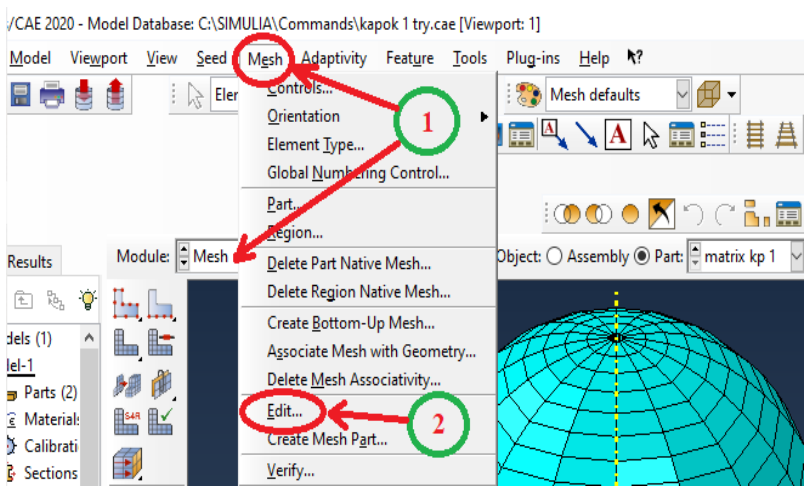

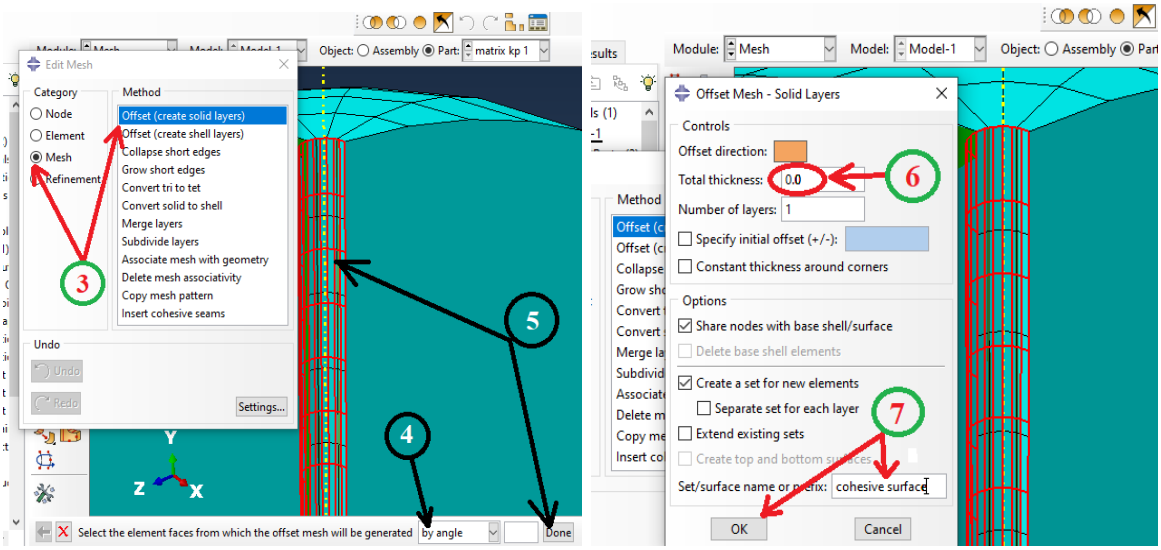

To create a cohesive element on the surface of the epoxy, which latter be the interface.

8. From the tabs on the top; select “mesh” and then “element type”
9. A new window will open, select the name we gave in step 7 and then click on continue
10. From the module, select a property and then "create section"
11. Select “other” from the categories listed and select the type to be “cohesive” then click on continue
12. Select material which we created in step 9 then select “ok”

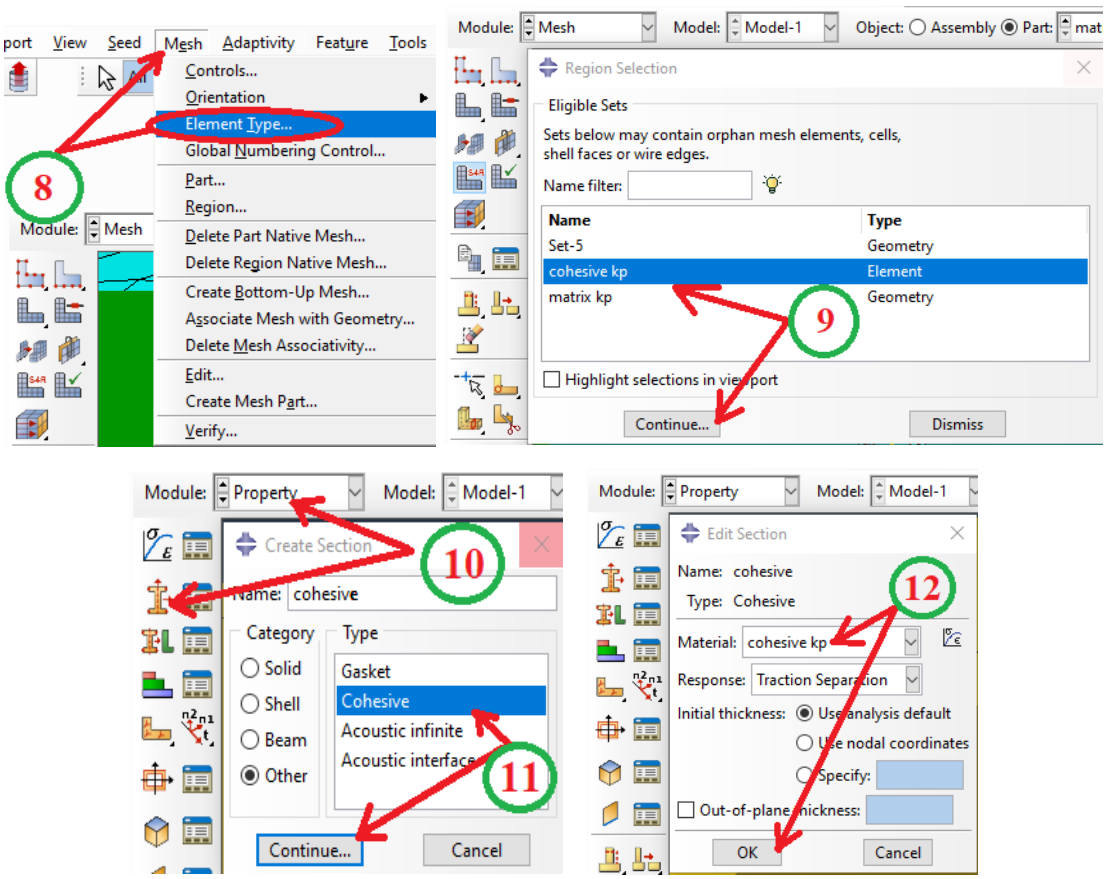

In order to assign material property to the cohesive section we created;

13. Select "assign the material property" from property under the module
14. Select the section as we have named it when creating a property by creating a material property, and the "continue"
15. From the window popped out, select the element library to be explicit, and select the family to be “cohesive” and then “ok”

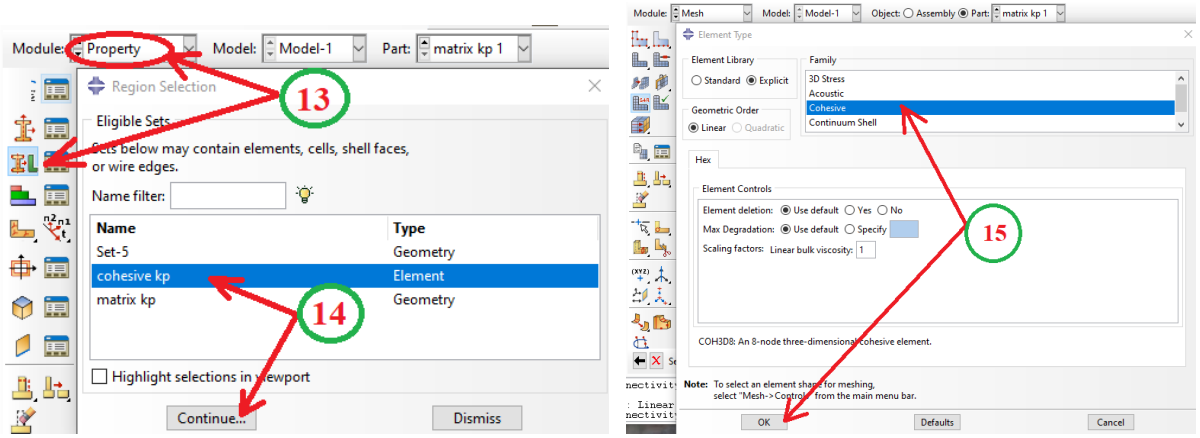

Note: After creating a cohesive layer and assigning a material property to it; we have to assemble the layer to the inner part of the epoxy which will later be the interface for fiber embedment.

Create step

1. Select "Step" under module select "step manager"
2. Create a step
3. Give name
4. Select "dynamic explicit"

   By clicking on "continue" a new window will pop out then;
5. Give time period (in this thesis, the time considered to pull the fiber out is 1 second)

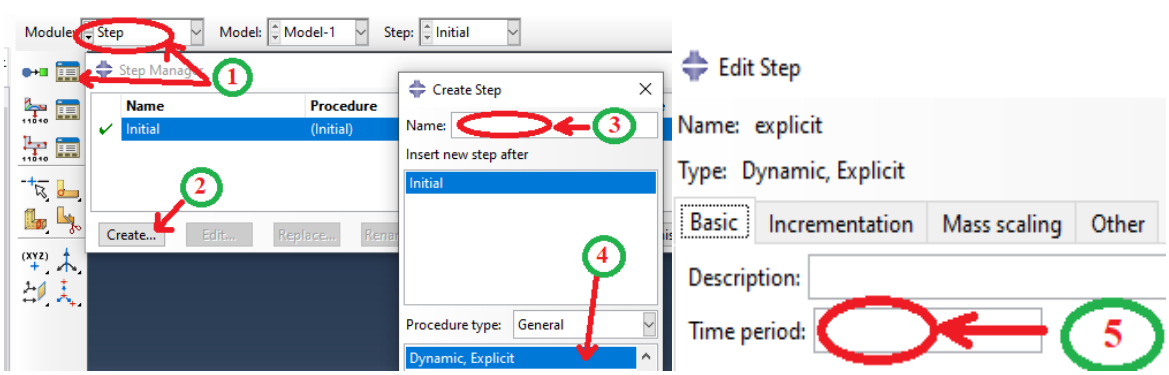

After giving the "Time period" value, give an "Amplitude" value and make it equal to what is given as a required amount of distance that we need to pull the fiber out, which is the value that we ought to give on the 8th step in "boundary condition" section. So that will be our amplitude distance.

Create a reference point

1. From the module; select interaction
2. Click on "R.P. (reference point)"
3. Select a datum point as a reference point (assign it some distance from the fiber along in the central axis of the fiber rod, in the direction to where it is going to be pulled) then press enter from the keyboard

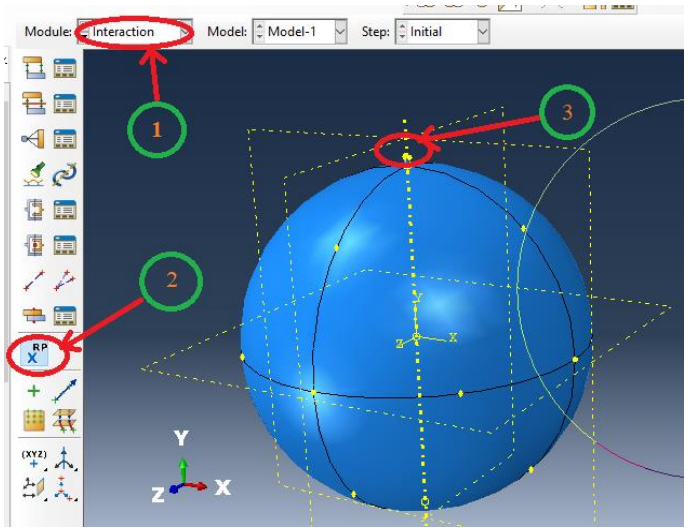

Create interaction

1. Select "interaction" from the module and click on create interaction
2. Create interaction
3. Select general contact (explicit) then click “continue”

   A new window will pop out to enable us to edit interaction and create interaction property
4. Click on the small Icon in "global property assignment" to create an interaction property
5. Give a name for the interaction on the newly opened window
6. Select "contact" from the types that are listed and then click on continue

   a window will pop out to edit the contact property

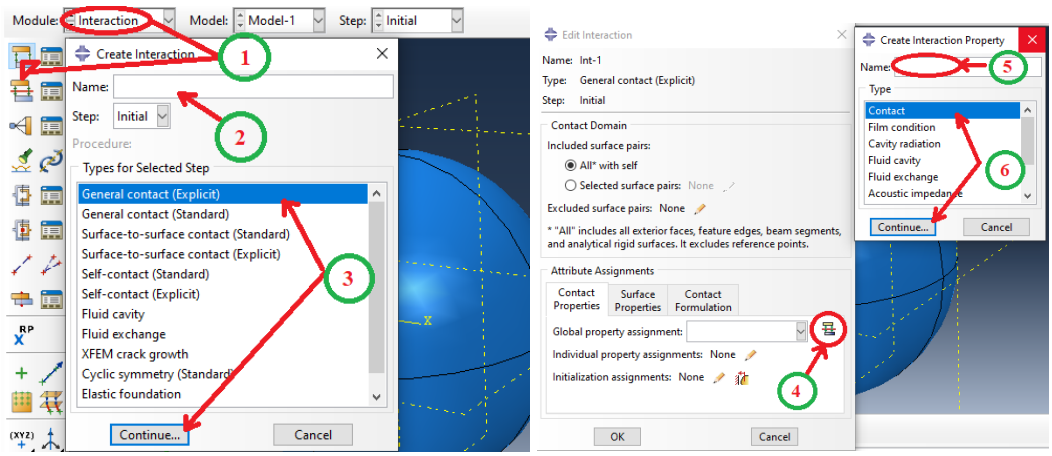

Tangential interaction:

7. Select the mechanical contact property
8. Then select tangential behavior
9. Enter coefficient of friction value

In the case of natural fiber, the coefficient of friction is 0.58 [72]

Cohesive interaction

10. Click on Mechanical
11. Then cohesive interaction
12. Set it as default if the stiffness matrix is not known

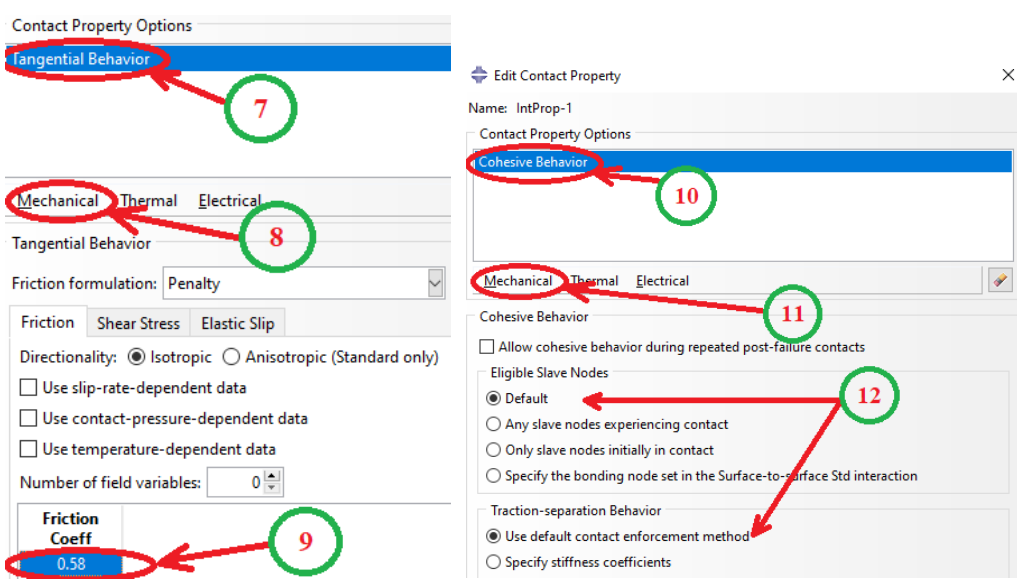

Note: Since stiffness matrix values of natural fiber are not available from the literature, I used a default cohesive interaction.

Boundary condition

1. Select "Load" from the module menu
2. Select “Create condition manager”
3. Click on "create"
4. Select "Mechanical" from the category
5. Give a name for the boundary condition

Boundary Condition 1: In order to pull the fiber out, we have to set condition 1

6. From the mechanical menu, select "Displacement/rotation"
7. Select the reference point
8. Give a value in the direction of the axis of the fiber

note: the given value describes how far the fiber has to be pulled-out

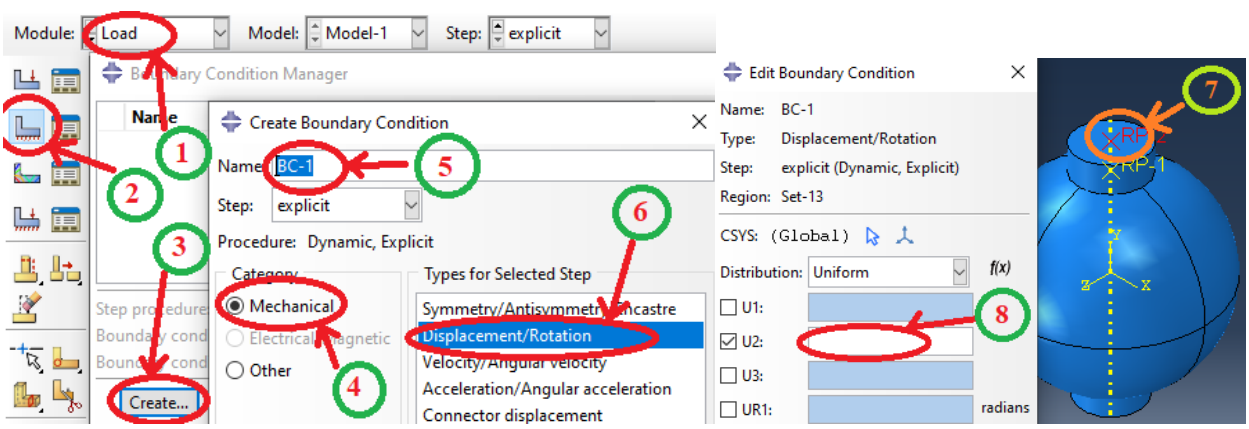

Boundary Condition 2: To fix the outer part of the epoxy

9. select symmetry/Antisymmetric/Encastre option
10. press shift and select multiple reference points around the equator
11. then select “Encastre (U1=U2=U3=UR1=UR2=UR3=0) so those points will be fixed as a rigid constraint

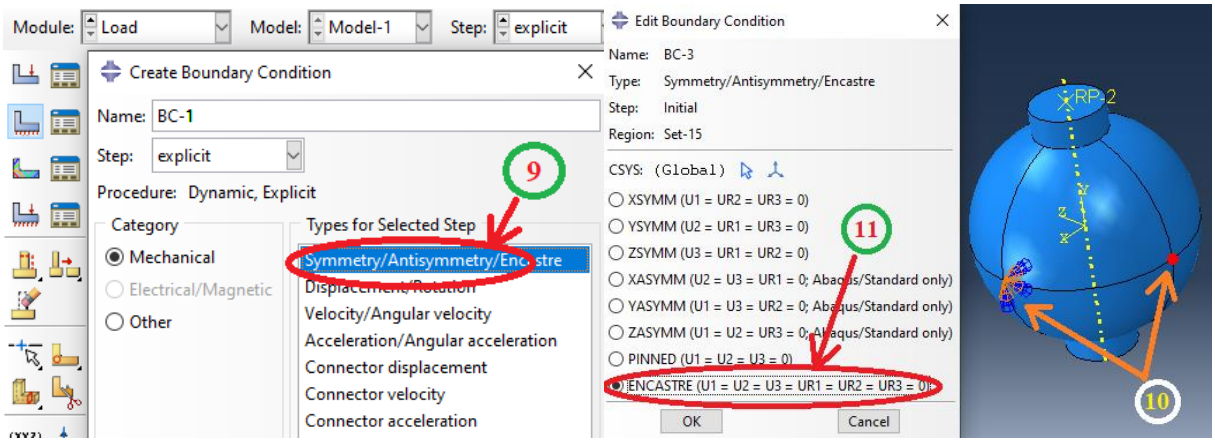

Mesh: Meshing is one of the key components to obtaining accurate results from an FEA model

1. select "Mesh" from the module
2. enter global size
3. apply

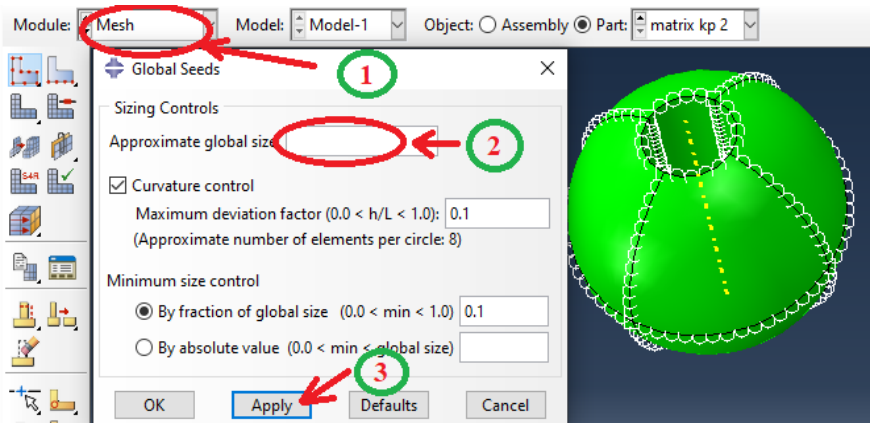

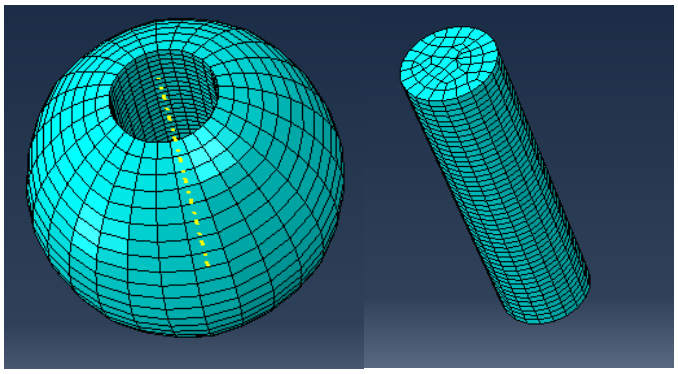

Note: a default type of element is used and and considereation of element size is different from one model to another and is dependent of the matrix and fiber size.

Assembly: this step is on assembling necessary parts before we create and run the job

1. Select “Assembly” from the module menu
2. Click on "Create instance"
3. From parts, select the desired parts to assemble
4. Apply

After we click on "Apply" there might be some miss-alignment so we have to drag, rotate and align parts accordingly to be assembled in the way it is supposed to be.

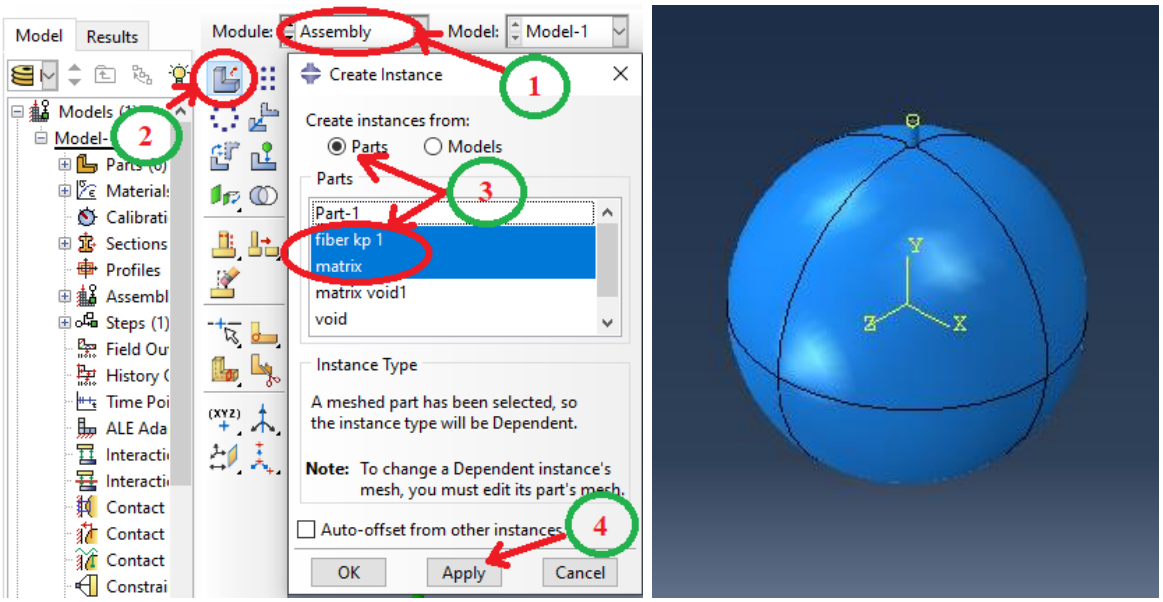

Job: this is the step where we submit what we have modeled to run

1. Select “job” from the module and then select "create job"
2. In the “create a job” window, select the model on which we want to run the job and then give a name for the job
3. Then click “continue”
4. On the "edit job" window, select "full analysis" if it is full analysis then click on "ok" to proceed to the next step
5. Select “job manager” from the list of icons on the left side
6. Then click “submit” so the job, which is the pulling out process, will start

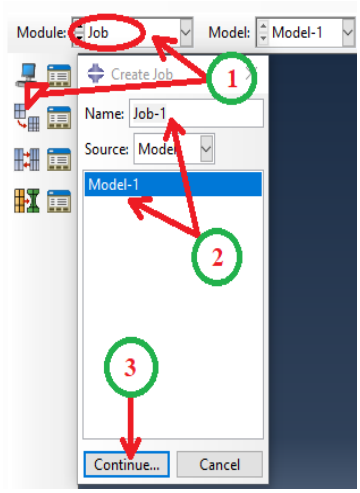

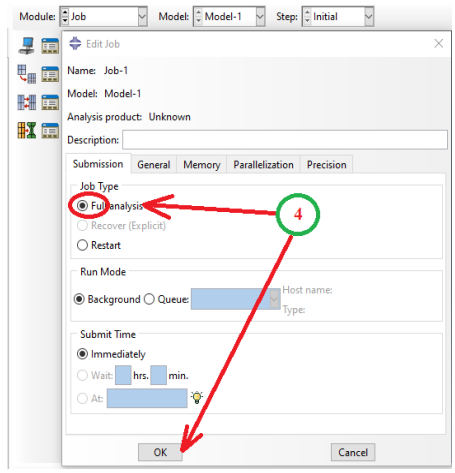

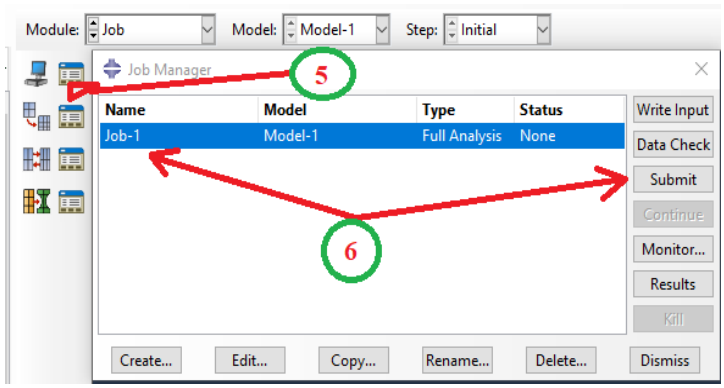

Result: in order to obtain results

1. Select virtualization from the module, then right-click on "XYData" then select "Create.."
2. Select “ODB field output” then continue
3. Select edit selection, then select the reference point and the plot

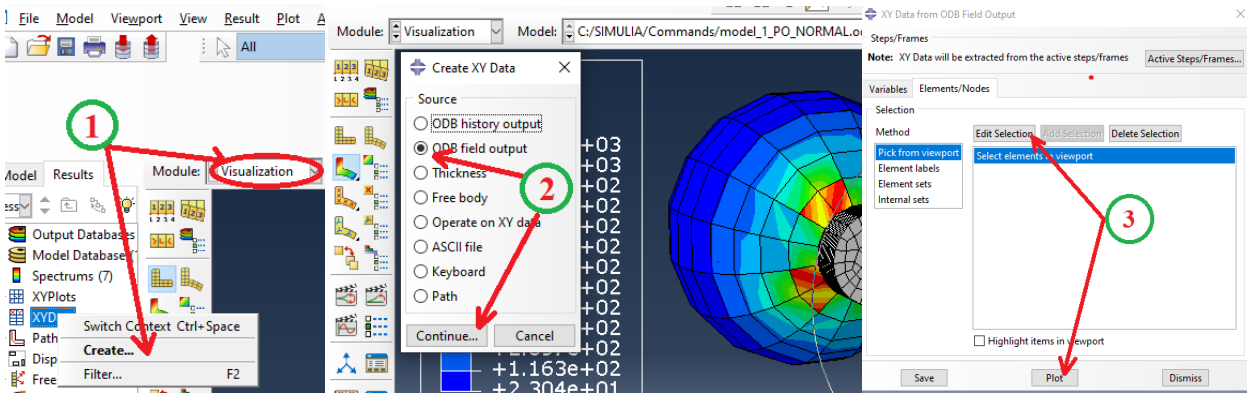

In order to get a force-displacement graph, from XYData, select operate on XY data and then combine (“displacement - time graph", "force-time graph")

Note: The maximum force in pulling out the fiber from its epoxy embedment can be obtained from force vs. time table.

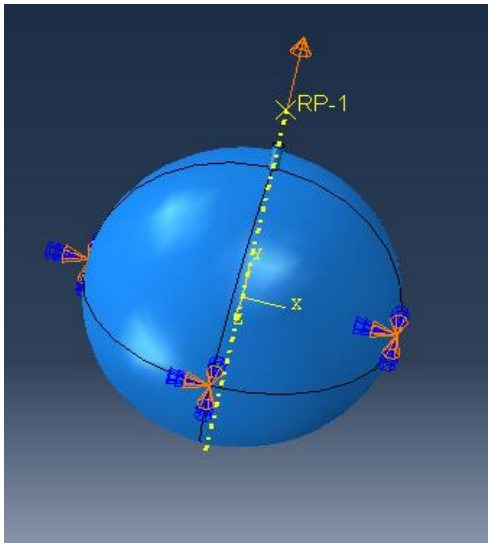

Figure 3.2: boundary fixation

3.3 ABAQUS 3D MODELING

3.3.1 Modeling

Before starting to define this or any model, we need to decide which system of units we will use. ABAQUS has no built-in system of units. So we cannot include names or labels when entering data in ABAQUS. All input data must be specified in consistent units. Some common systems of consistent units are shown in the table 3. [81]

Table 3 Consistent units

Quantity	SI	SI (mm)	US Unit (ft)	US Unit (inch)
Length	mm	mm	ft	in
Force	N	N	lbf	lbf
Mass	kg	tonne(10^3 kg)	$slug$	$lbf s^2/in$
Time	s	s	s	s
Stress	Pa (N/m^2)	MPa (N/mm^2)	lbf/ft^2	psi (lbf/in^2)
Energy	J	$MJ(10^{-3}\ J)$	ft lbf	in lbf
Density	kg/m3	tonne/mm^3	slug/ft^3	lbf s^2/in^4

The SI system of units is used throughout this guide. Users working in the systems labeled "US Unit" should be careful with the units of density; often the densities given in handbooks of material properties are multiplied by the acceleration due to gravity. [81]

From the table of consistent units, I choose the SI unit system to feed dimensions and parameters to ABAQUS. The diameter and length of the fibers are taken from the literature [70] [71] as is described in Chapter 3.

So as it is stated in table 3, the length has to be converted to mm as well as the Elastic modus to Pascal and the Density to kg/m^3 in order to feed ABAQUS.

3.3.2 Void formation

There is no data on the position and volume distribution of void in a single fiber-epoxy matrix so the void is taken randomly by varying its size. Since the reason void is considered in some models in this study is in the intention of studying if the presence of any void does have an effect on the IFSS on fiber-epoxy matrix, it is not to compare with what is experimentally obtained.

The ratio of the void is not something found with some specific proportionality range of volume in literature. It can be too small to be detected or too huge that will leave the fiber interface be opened.

So To study the effect of the presence of void on the interface area between the matrixes an epoxy, which is the main objective of considering void on the interface, an elliptical void is taken with its Minor diameter is 20% of the length of the embedded length of the fiber on the epoxy, for four models, which the two voids will cause the interface to be 30% to 40% opened.

In this paper, Void on some models is put in order only to study the effect of the presence of void on the IFSS or to see if the presence of void and the change in the size of void could result in any change on the IFSS value.

3.4 ABAQUS 3D Models

This section is about the 3D modeling parameters of different models. Twelve 3D models were modeled, six for each fiber, by changing sizes such as fiber length, diameter, and void exposed area.

The archetypical models are model 1.1 for pineapple and model 3.1 for Kapok, which are modeled by using size parameters found from the works of the literature surveyed. Those are the parameters put under table 1. The other models are the replica of it by varying the length of fiber, diameter and putting some void on the interface. The mechanical properties are the same as the archetypical since it's not only the case that it is not the objective but also changing the fiber size will not change the mechanical properties of the fiber such as its young's modulus and density value.

The models and corresponding changes were taken on the archetypical are listed in table 4.

Table 4: Models with corresponding changes made

Fiber	3D Model no		Variation/change on	Ø (μm)	EL (mm)
Pineapple	1	1.1	**Taking parameters from table 1**	48	3
		1.2	The presence of void on 1.1		
	2	2.1	The embedded length of 1.1	48	0.1
		2.2	The Ø of 2.1	36	
		2.3	The presence of void on 2.1	48	
		2.4	The void size of 2.3		
Kapok	3	3.1	**Taking parameters from table 1**	33	1
		3.2	The Ø of 3.1	45	
		3.3	The presence of void on 3.1	33	
		3.4	The void size of 3.3		
	4	4.1	The embedded length of 3.1	33	0.1
		4.2	The presence of void on 4.1		

3.4.1 Pineapple

Model 1.1:

Diameter 48 µm = $4.8e^{-5}$m

Length 3.14 mm = $3.14e^{-3}$m

Epoxy droplet = $3e^{-3}$m in Ø

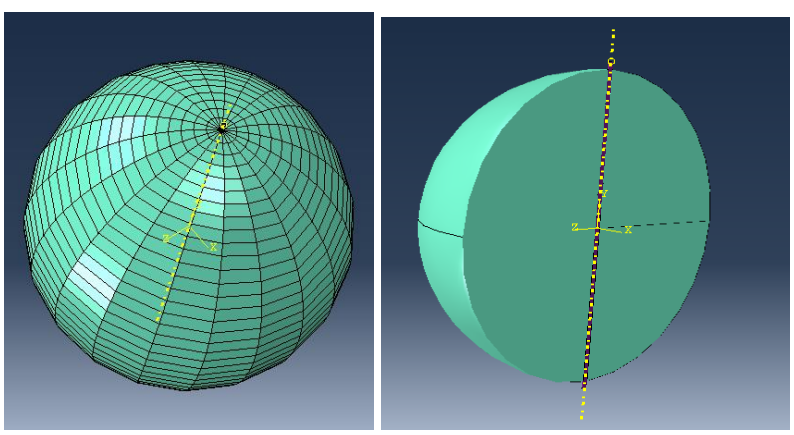

A B

Figure 3.3: Meshed 3D view (A), and sectional view (B) of model 1.1

Model 1.2 (model 1.1 with void)

Supposing there are two elliptical voids with the dimension of:

Minor diameter: $6e^{-4}$m in the y-axis

Major diameter: $18e^{-4}$m across horizontal

Putting their center equally apart by $12e^{-5}$m from center | origin of the epoxy droplet sphere and subtracted from epoxy to result in an elliptical void as shown in figure 28.

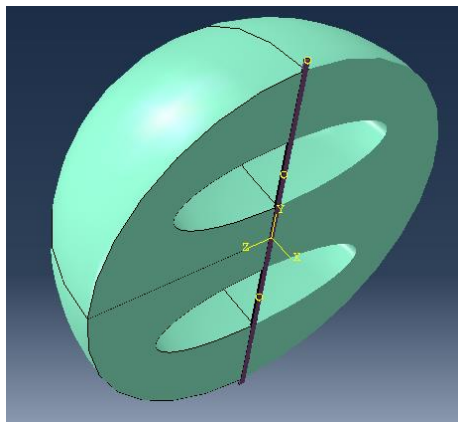

Figure 3.4: Sectional view of model 1.1 with the presence of two elliptical voids

Model 2.1:

Diameter 48 µm = $4.8e^{-5}$m

Length 0.12 mm = $1.2e^{-4}$m

Epoxy droplet = $1e^{-4}$m in Ø

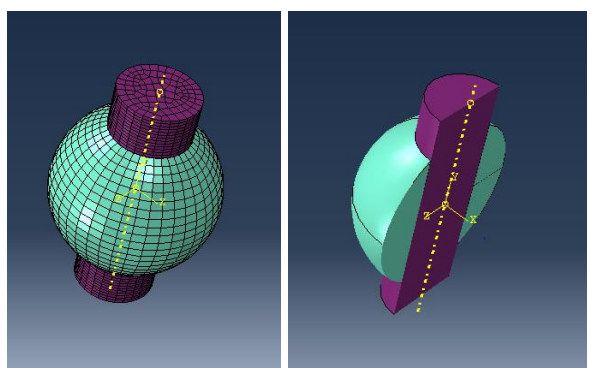

A B

Figure 3.5: Meshed 3D view (A) and sectional view (B) of model 2.1

Model 2.2 (model 2.1 with change in fiber diameter)

Diameter 36 µm = $3.6e^{-5}$m

Length 0.12 mm = $1.2e^{-4}$m

Epoxy droplet = $1e^{-4}$m in Ø

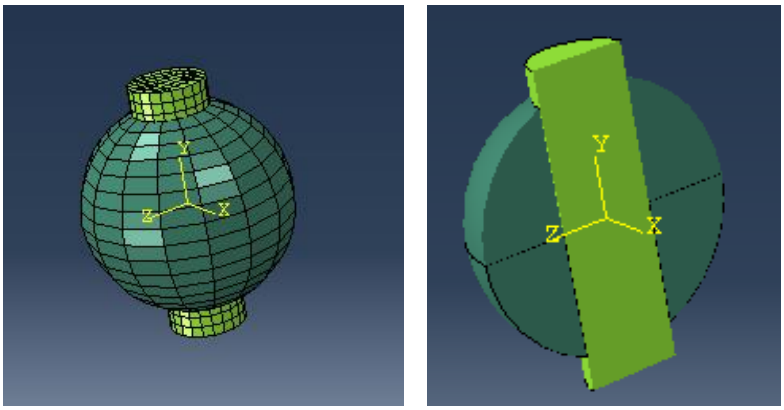

A B

Figure 3.6: Meshed 3D view (A) and sectional view (B) of model 2.2

Model 2.3: (model 2.1 with void)

Supposing there are two elliptical voids with a dimension of:

Minor diameter: $2e^{-5}$m in the y-axis and Major diameter: $6e^{-5}$m across horizontal

Putting their center equally apart by $4e^{-5}$m from center | origin of the epoxy droplet sphere and subtracted from epoxy to result in an elliptical void as shown in the figure 31.

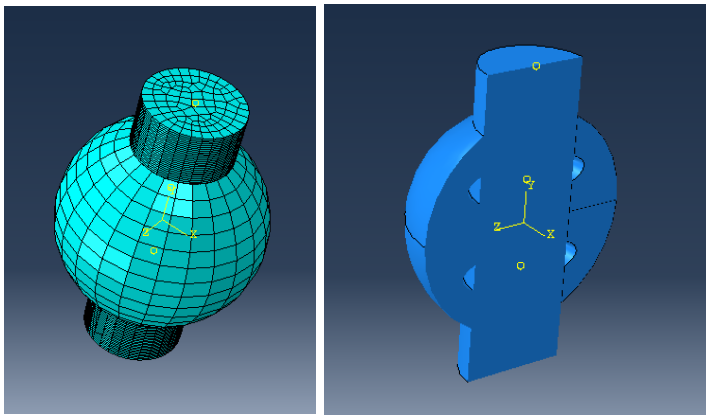

Figure 3.7: 3D full and Sectional view of model 2.1 with the presence of two elliptical void

Model 2.4 (model 2.3 with void ratio change)

For Minor diameter

10% of its embedded length is $1e^{-4} * \frac{1}{10} = 1e^{-5}$m

So by making the Minor diameter of the elliptical void be $1e^{-5}$m and by making only one void. It is modeled as such only to compare and study the effect of the change of void ratio on the interfacial shear strength value of the same epoxy size and the same fiber diameter.

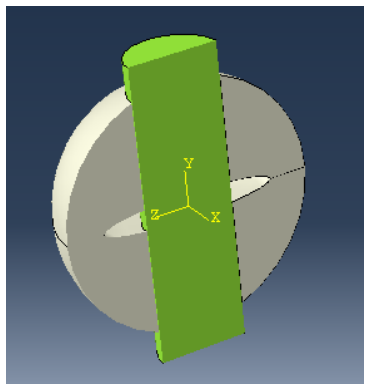

Figure 3.8: sectional view model 2.4 having a small void

3.4.2 Kapok

Model 3.1:

Diameter 33 µm = 3.3 e^{-5}m

Length 1.14 mm = $1.14e^{-3}$m

Epoxy droplet = $1e^{-3}$m in Ø

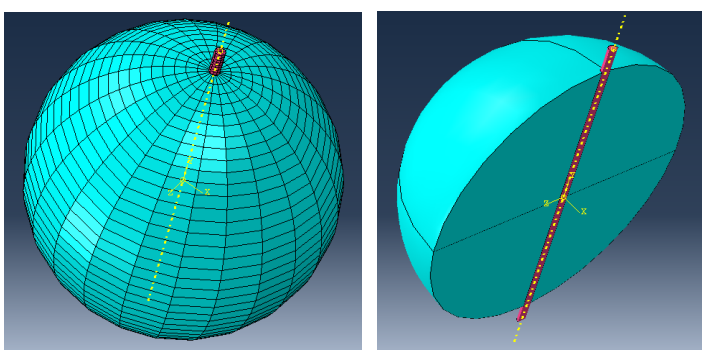

A B

Figure 3.9: Meshed 3D view (A) and sectional view (B) of model 3.1

Model 3.2 (model 3.1 with change in fiber diameter)

Diameter 45 µm = $4.5e^{-5}$m

Length 1.14 mm = $1.14e^{-3}$m

Epoxy droplet = $1e^{-3}$m in Ø

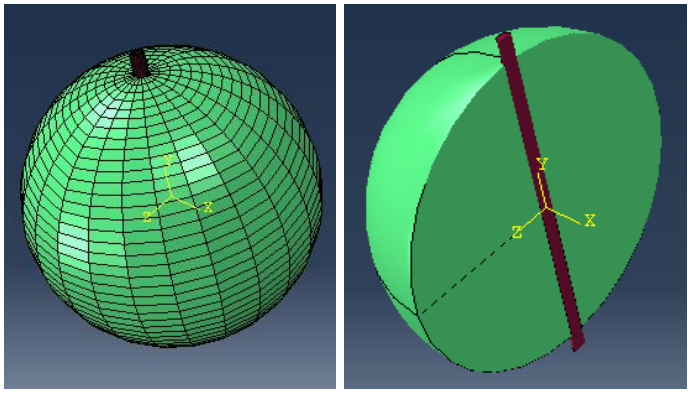

A B

Figure 3.10: Meshed 3D view (A) and sectional view (B) of model 3.2

Model 3.3 (model 3.1 with void)

Two elliptical voids with a dimension of

Minor diameter: $2e^{-4}$m in the y-axis

Major diameter: $6e^{-4}$m across horizontal

Putting their center equally apart by $4e^{-4}$m from center | origin of the epoxy droplet sphere and subtracted from epoxy to result in an elliptical void as shown in the figure 35.

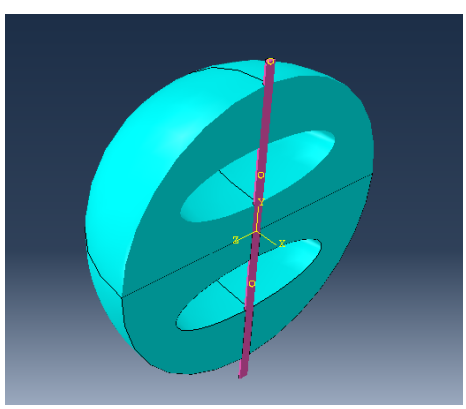

Figure 3.11: Sectional view of model 3.3, (model 3.1 with the presence of two elliptical voids)

Model 3.4 (model 3.3 with void ratio change)

Embedded length of the fiber is = the diameter of the epoxy = $1e^{-3}m$

45% of $1e^{-3}m = 0.45\%$

So 3 voids, each is having 0.15% of the total embedded length which is $0.15e^{-3}m$ as the Minor diameter is subtracted from the epoxy as shown 36.

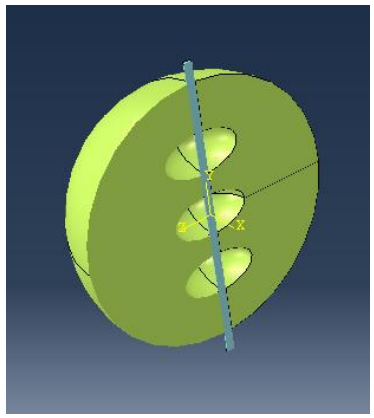

Figure 3.12: 3D meshed Sectional view of model 3.4

Model 4.1:

Diameter 33 µm = $3.3e^{-5}$m

Length 0.14 mm = $1.4e^{-4}$m

Epoxy droplet = $1e^{-4}$m in Ø

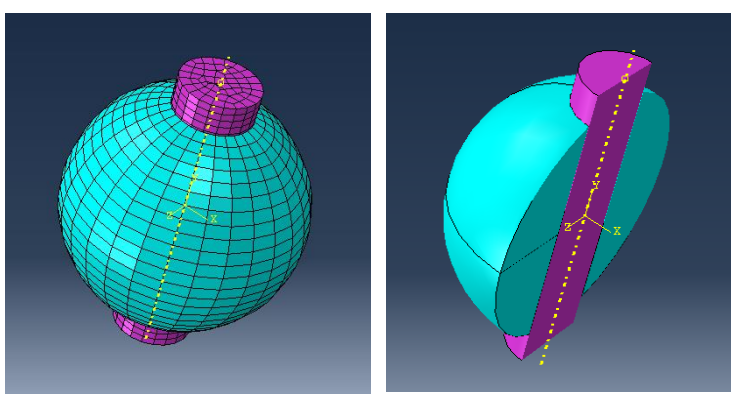

A B

Figure 3.13: Meshed 3D view (A) and sectional view (B) of model 4.1

Model 4.2 (model 4.1 with void)

Two elliptical voids with Minor diameter: $2e^{-5}$m in the y-axis and Major diameter: $6e^{-5}$m across

Putting their center equally apart by $4e^{-5}$m from center; origin of the epoxy droplet sphere and subtracted from epoxy to result in an elliptical void as shown in figure 38.

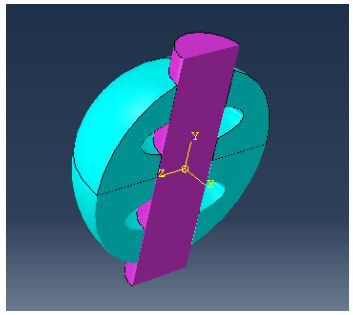

Figure 3.14: Sectional view of model 4.2 with the presence of two elliptical voids

4. CHAPTER FOUR: RESULT AND DISCUSSION

Shear strength is the strength of a material or component against the type of yield or structural failure when the material or component fails in shear. A shear load is a force that tends to produce a sliding failure on a material along a plane that is parallel to the direction of the force. In structural and mechanical engineering, the shear strength of a component is important for designing the dimensions and materials to be used for the manufacture or construction of the component.

Shear strength is calculated by dividing the force that causes shear to the area of the shear plane.

$$\tau = \frac{F}{A} \tag{4.1}$$

Where:

F is Force and

A is area

The area to be sheared is the contact surface between the embedded fiber and epoxy; which is the outer surface of the net embedded length. So since the fiber is cylindrical, the contact surface is the total lateral surface area of the fiber in its net embedded part.

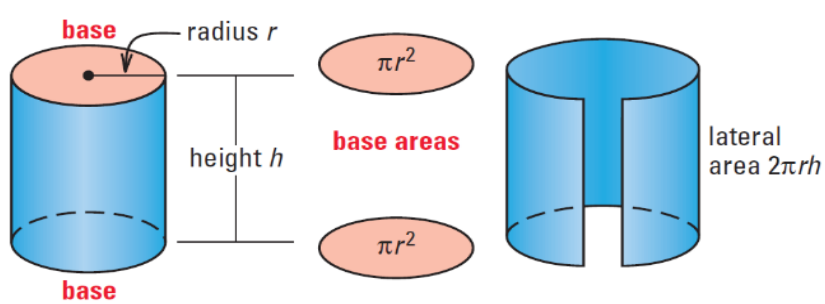

Figure 4.1: Surface area of a cylinder [75]

The lateral surface area of a cylinder is given by:

$$A_{cl} = 2\pi r h \tag{4.2}$$

In our case, the height is the net embedded length of the fiber, which is in contact with the epoxy, so the formula is rewritten as:

$$A_c = 2\pi r l_e \tag{4.3}$$

Where:

l_e= the net embedded length of the fiber

r= radius of the fiber

A_c= contact surface area

In case of having void gapping the lateral surface of the fiber is to contact epoxy.

Net contact surface area = lateral surface of the embedded fiber – uncovered area due to void

$$A_c = 2\pi r h_{te} - 2\pi r h_v \tag{4.4}$$

And since $2r = d$

$$A_c = \pi . d_f . l_e = \pi . d_f . (h_{te} - h_v) \tag{4.5}$$

Where:

l_e= the net embedded length of the fiber

h_{te} = total embedded fiber length

h_v = total void exposed fiber length

d_f= diameter of the fiber

d_f = diameter of fiber

A_c = contact surface area

By substituting eq.4.1 in eq.4.5 we get;

The interfacial shear strength τ_{IFSS} [54]

$$\tau_{IFSS} = \frac{F_{max}}{\pi . d_f . l_e} \tag{4.6}$$

Where:

F_{max} = the maximum value of pull-out force.

d_f = the diameter of a single fiber.

l_e = the embedded length of the microdroplet.

And in case of the presence of void, equation 4.6 can be modified as

$$\tau_{IFSS} = \frac{F_{max}}{\pi . d_f . (h_{te} - h_v)} \tag{4.7}$$

4.1 Results and Discussions

We can obtain the exact measure of net embedded length by measuring right on Abaqus; the maximum force is obtained from force-time table on the result. The diameter of the fiber is taken from table 4. Then by substituting those values on equation 4.6, the Interfacial shear strength is calculated as such:

Model 1.1:

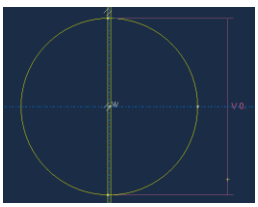

$= 0.00299958330439413 \cong 3e^{-3} = l_e$

From table 3:

$$d_f = 48\mu m = 4.8e^{-5}m$$

By combining force – time to displacement – time graph, a force-displacement graph is:

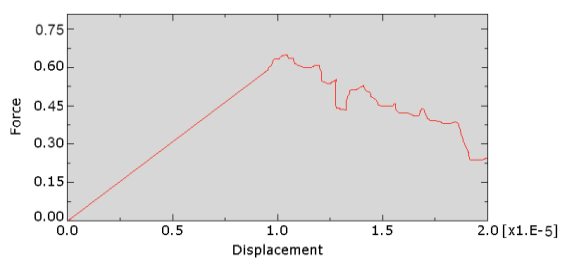

Figure 4.2: Force - amplitude displacement of model 1.1

$$F_{max} = 0.6352 = 6.3e^{-1}N$$

By substituting those values on the interfacial shear strength formula: we get

$$\tau_{IFSS} = \frac{6.3e^{-2}N}{\pi * 4.8e^{-5}m * 3e^{-3}m} = 1.393\ MPa$$

Net fiber-epoxy contact surface area

$$A_c = 2\pi r l_e = 2\pi * 2.4e^{-5} * 3e^{-3}$$

$$A_c = 4.52e^{-7} m^2$$

Model 1.2: (model 1.1 with void)

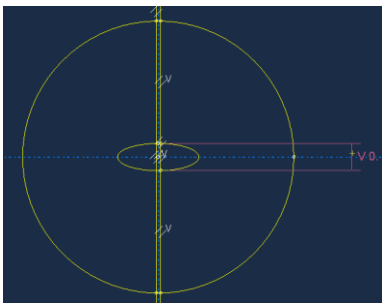

$= 0.00029957302949364 * 2 = 5.991e^{-4}$

So the net embedded length is $l_e \cong 3e^{-3} - 5.991e^{-4} \cong 2.4e^{-3} m$

From table 3: $d_f = 48\mu m = 4.8e^{-5} m$

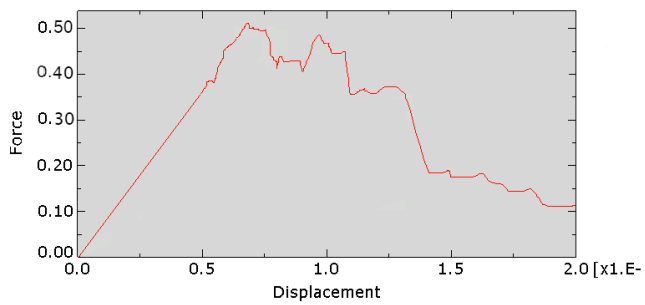

Figure 4.3: Force - amplitude displacement of model 1.2

$$F_{max} = 0.52 = 5.2e^{-1} N$$

By substituting those values on the interfacial shear strength formula: we get

$$\tau_{IFSS} = \frac{5.2e^{-1} N}{\pi * 4.8e^{-5} * 2.4e^{-3}} = 1.437\ MPa$$

Net fiber-epoxy contact surface area

$$A_c = 2\pi r l_e = 2\pi * 2.4e^{-5} * 2.4e^{-3}$$

$$A_c = 3.62e^{-7} m^2$$

Discussion on the result of model 1.1 and 1.2

From the values obtained of pineapple fiber of 3mm embedded in epoxy, the interfacial area of $4.52e^{-7}m^2$ the Maximum force needed to pull out the fiber is $6.3e^{-2}\ N$ and the interfacial shear strength is $1.393\ MPa$. While the interfacial contact area decreased by 20% to $3.62e^{-7}m^2$ due to the presence of two elliptical voids, the Force also decreased by 21% to $5.2e^{-2}\ N$ but the IFSS remains the same, only slightly increased by 2% to $1.43\ MPa$.

- From this, we can say that the change in length and the presence of void which results in a change in the area directly affects the force needed to pull out but that has a negligible effect on the interfacial shear strength.

Model 2.1:

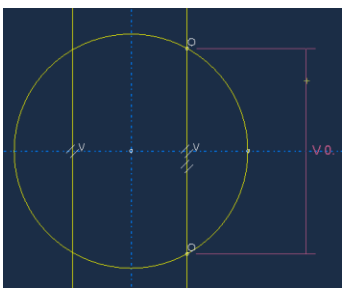

$= 8.77268487978452e^{-5}$; $l_e \cong 8.7727e^{-5}m$

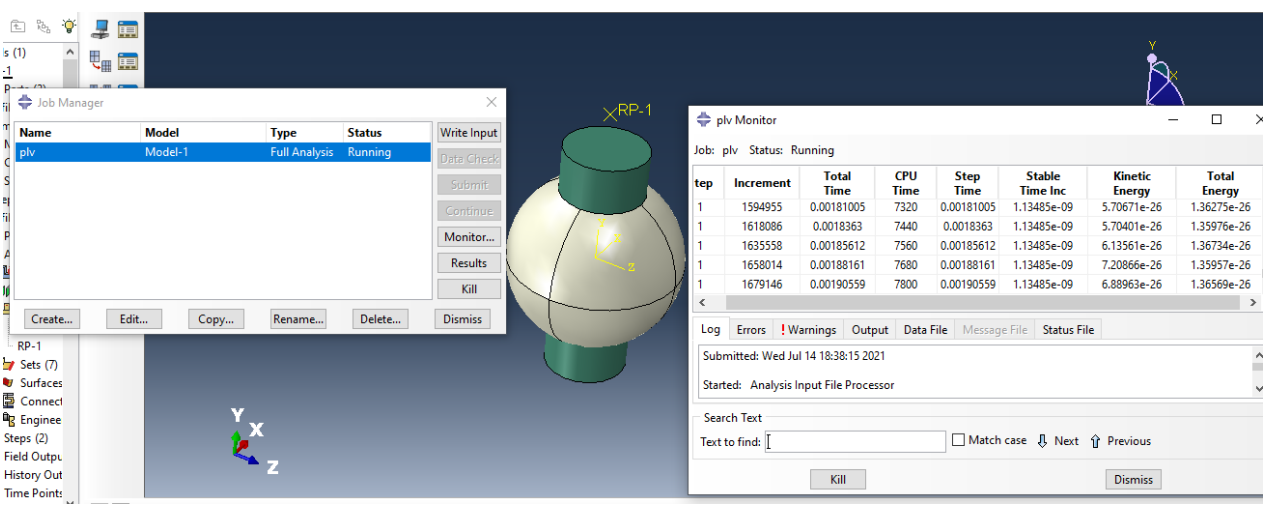

Figure 4.4: Job running of model 2.1

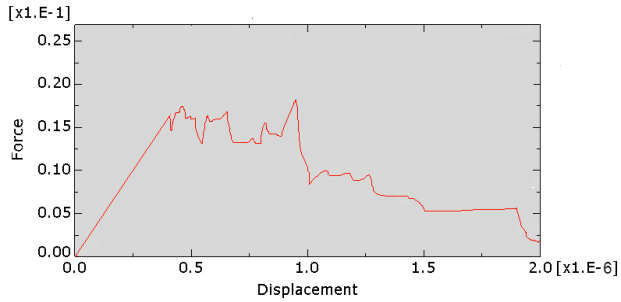

Figure 4.5: Force - amplitude displacement of model 2.1

$$F_{max} = 0.185e^{-1} = 1.85e^{-2}N$$

From table 3; $d_f = 48\mu m = 4.8e^{-5}m$

By substituting those values on the interfacial shear strength formula: we get

$$\tau_{IFSS} = \frac{1.85e^{-2}N}{\pi * 4.8e^{-5} * 8.7727e^{-5}} = 1.398\ MPa$$

Net fiber-epoxy contact surface area

$$A_c = 2\pi * 2.4e^{-5} * 8.7727e^{-5} = 1.32e^{-8}m^2$$

Model 2.2 (model 2.1 with change in fiber diameter)

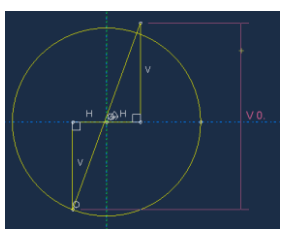

$\cong 9.94e^{-5} = l_e$

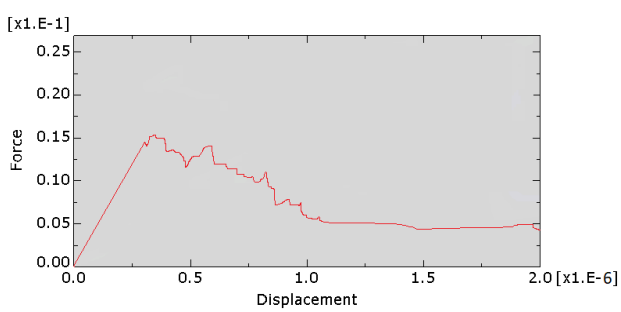

Figure 4.6: Force - amplitude displacement of model 2.2

From Table 3: $d_f = 36\mu m = 3.6e^{-5}m$

By substituting those values on the interfacial shear strength formula: we get

$$\tau_{IFSS} = \frac{1.55e^{-2}N}{\pi * 3.6e^{-5}m * 9.94e^{-5}m} = 1.379\ MPa$$

Discussion on results from model 2.1 and model 2.2

Changing the diameter size of the embedded fiber from 3 mm to 0.1 mm, by one thirteenth, the IFSS values goes from $1.398\ MPa$ to $1.379\ MPa$, decreased by 1.36%. Even if the diameter is minimized thirteen times only to yield a small change on the IFSS, we can say that change in diameter do affect the IFSS in a direct relational way.

Model 2.3: (model 2.1 with void)

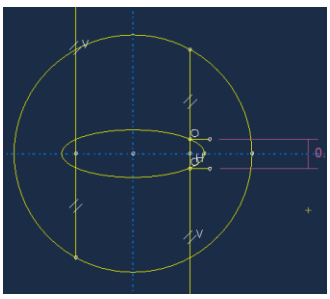

$= 1.21756456792355e^{-5} * 2 \cong 2.43513e^{-5}$

$$l_e \cong 8.7727e^{-5} - 2.43513e^{-5} = 6.33757e^{-5}m$$

From table 3; $d_f = 48\mu m = 4.8e^{-5}m$

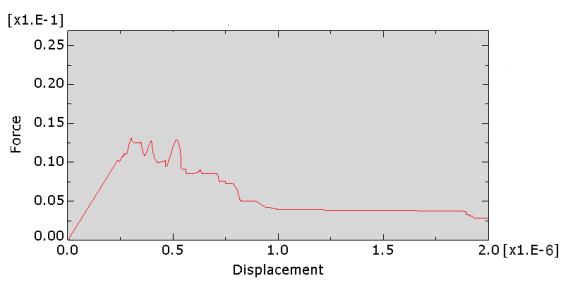

Figure 4.7: Force - amplitude displacement of model 2.3

$$F_{max} = 0.135e^{-1} = 1.35e^{-2}N$$

By substituting those values on the interfacial shear strength formula: we get

$$\tau_{IFSS} = \frac{1.35e^{-2}N}{\pi * 4.8e^{-5} * 6.33757e^{-5}m} = 1.4126\ MPa$$

Net fiber-epoxy contact surface area

$$A_c = 2\pi r l_e = 2\pi * 2.4e^{-5} * 6.33757e^{-5}$$

$$A_c = 1.84e^{-9}m^2$$

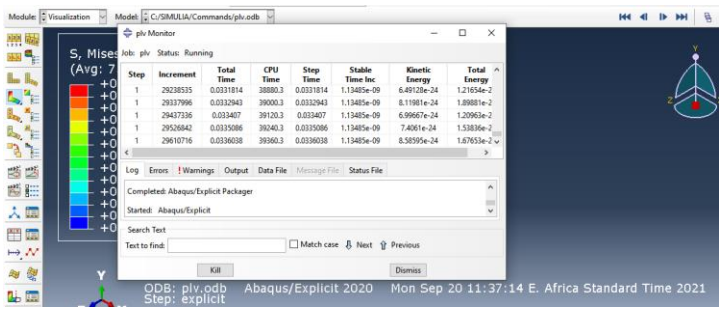

Figure 4.8: Model 2.3 during job running with time incrementation of 10^{-9}

Discussion from the result of models 2.1 and 2.3

Pineapple fiber of 1mm embedded in epoxy, the interfacial area of $1.32e^{-8}m^2$ the Maximum force needed to pull out the fiber is $1.85e^{-2}\ N$, and the interfacial shear strength is$1.397\ MPa$. While the interfacial contact area decrease by 38% to $9.56e^{-9}m^2$ due to the presence of two elliptical voids, unlike the first two models, the Force inversely increases by 41% to $5.2e^{-2}\ N$ but the IFSS remains, only slightly increased by 1.4% to $1.416\ MPa$.

- From this, we can say that the change in length and the presence of void which results in a change in area inversely affects the force needed to pull out but that has almost no effect on the interfacial shear strength.

Model 2.4 (model 2.3 with void ratio change)

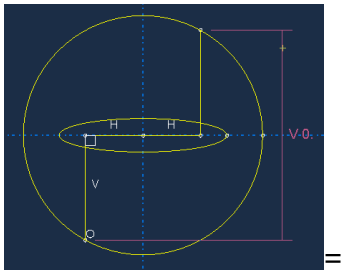

$= 8.77e^{-5}$

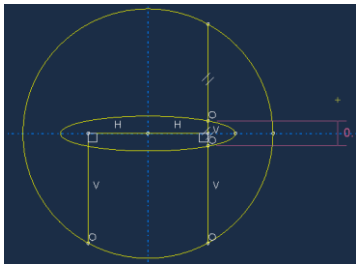

$= 0.99e^{-5}$

The net embedded length is $8.77e^{-5} - 0.99e^{-5} \cong 7.78e^{-5}$; $l_e \cong 7.78e^{-5}m$

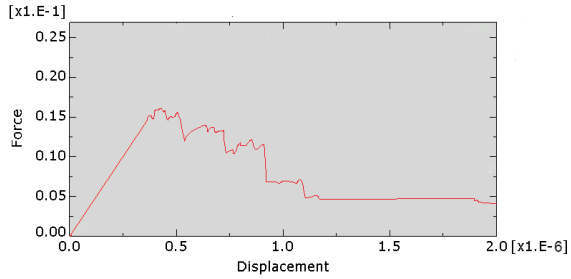

Figure 4.9: Force - displacement graph of model 10

$$F_{max} = 0.164e^{-1} = 1.64e^{-2}N$$

By substituting those values on the interfacial shear strength formula: we get

$$\tau_{IFSS} = \frac{1.64e^{-1}N}{\pi * 4.8e^{-5} * 7.78e^{-5}m} = 1.398\ MPa$$

Discussion on 2.4 and 2.3

Decreasing the void on the interface decreases the IFSS from 1.429 MPa to 1.398 MPa which is about 1.0335%; so changing void size affects IFSS directly.

Model 3.1:

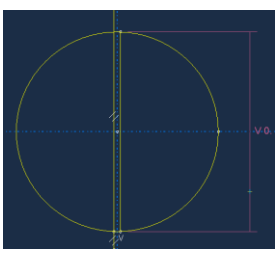

$= 0.000999455351679103 \cong 1e^{-3}m;\ l_e \cong 1e^{-3}m$

From table 3: $d_f = 33\mu m = 3.3e^{-5}m$

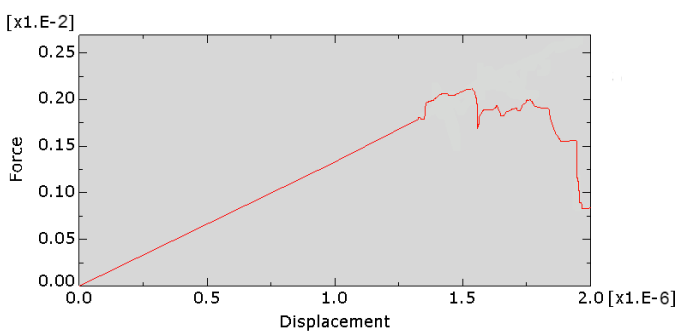

Figure 4.10: Force - displacement graph of model 3.1

$$F_{max} = 0.214e^{-2} = 2.1e^{-3}N$$

By substituting those values on the interfacial shear strength formula: we get

$$\tau_{IFSS} = \frac{2.1e^{-3}N}{\pi * 3.3e^{-5}m * 1e^{-3}m} = 0.02\ MPa$$

Net fiber-epoxy contact surface area

$$A_c = 2\pi r l_e = 2\pi * 1.65e^{-5} * 1e^{-3} = 1.04e^{-7}m^2$$

Model 3.2 (model 3.1 with change in fiber diameter)

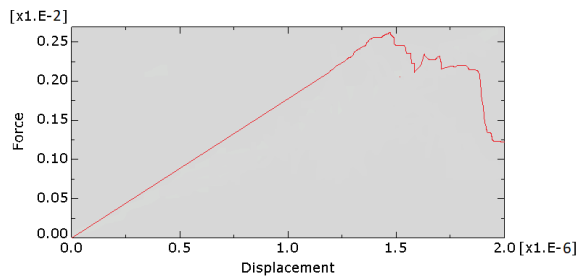

Figure 4.11: Force - amplitude displacement of model 3.2

Embedded length 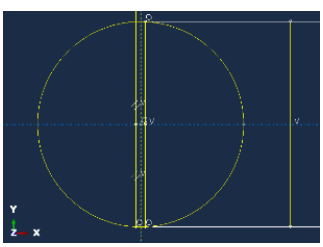 $= 0.9e^{-3}m$

$$\tau_{IFSS} = \frac{2.7e^{-3}N}{\pi * 4.5e^{-5} * 0.9e^{-3}} = 21226.415 = 0.0212\ MPa$$

$$A_c = 2\pi r l_e = 2\pi * 2.25e^{-5} * 0.9 = 1.27e^{-7}m^2$$

Discussion on 3.2 and 3.1

Changing the diameter size of the embedded fiber from 3 mm to 0.1 mm, by one thirteenth, the IFSS values goes from 1.398 MPa to 1.379 MPa, decreased by 1.56%. Even if the diameter is minimized thirteen times only to yield a small change on the IFSS, we can say that change in diameter do affect the IFSS in a direct relational way.

Model 3.3: (model 3.1 with void)

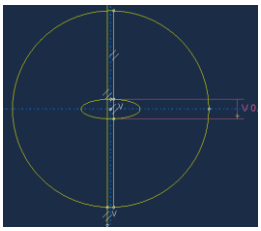

$= 9.93931587182941e^{-5} * 2 \cong 1.988e^{-4}$

$$l_e \cong 1e^{-3} - 1.988e^{-4} = 8.012e^{-4}m$$

Net fiber-epoxy contact surface area

$$A_c = 2\pi * 1.65e^{-5} * 8.012e^{-4} = 8.31e^{-8}m^2$$

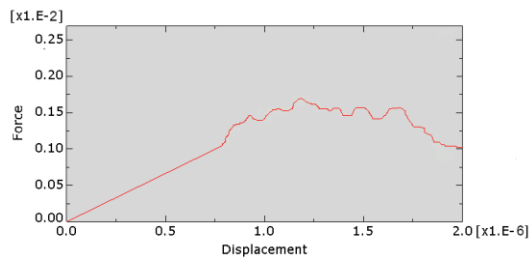

Figure 4.12: Force - amplitude displacement of model 3.3

$$F_{max} = 0.174e^{-2} = 1.74e^{-3}N$$

From table 3: $d_f = 33\mu m = 3.3e^{-5}m$

By substituting those values on the interfacial shear strength formula: we get

$$\tau_{IFSS} = \frac{1.74e^{-3}N}{\pi * 3.3e^{-5}m * 8.012e^{-4}m} = 0.021\ MPa$$

Discussion from the result of models 3.1 and 3.3

For Kapok fiber of 1mm embedded in epoxy, the interfacial area of $1.04e^{-7}m^2$ the Maximum force needed to pull out the fiber is $2.1e^{-3}\ N$ and the interfacial shear strength is $0.02\ MPa$. While the interfacial contact area decreased by 25% to $8.31e^{-8}m^2$ due to the presence of two elliptical voids, the Force also decreased by 21% to $1.74e^{-3}\ N$ but the IFSS remains the same, only slightly increased by 5% to $0.021\ MPa$.

- The change in length and the presence of void directly affects the force needed to pull out but that has a very small effect on the interfacial shear strength.

Model 3.4 (model 3.3 with void ratio change)

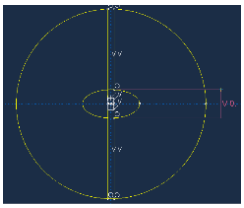 $= 0.149e^{-3} * 3 = 0.447e^{-3}$ 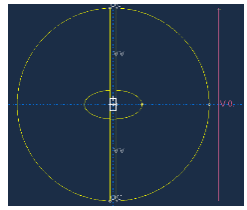 $= 0.999e^{-3}$

Net embedded length = $0.999e^{-3} - 0.447e^{-3} = 0.552e^{-3}m$

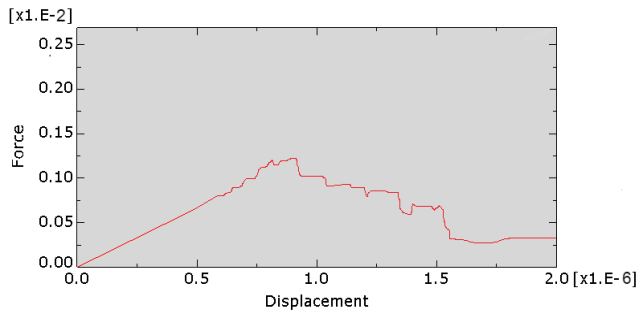

Figure 4.13: Force - amplitude displacement of model 3.4

$$\tau_{IFSS} = \frac{1.25e^{-3}N}{\pi * 3.3e^{-5}m * 0.552e^{-3}m} = 0.022\ MPa$$

Discussion on 3.4 and 3.3

Increasing void on the interface increases the IFSS from $0.021\ MPa$ to $0.022\ MPa$, around 4.76% increments. We can say that the more there is a void on the interface, the stronger to pull the fiber out.

Model 4.1:

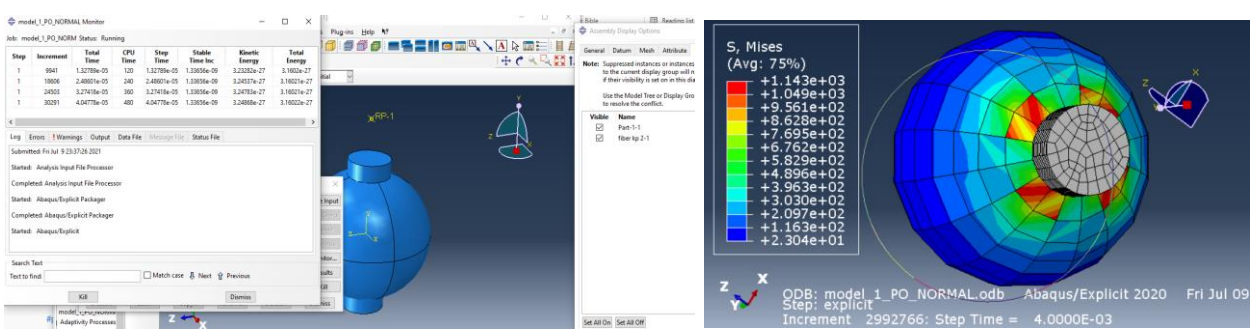

A B

Figure 4.14: screenshot of job running (A) and executed result in virtualization (B)

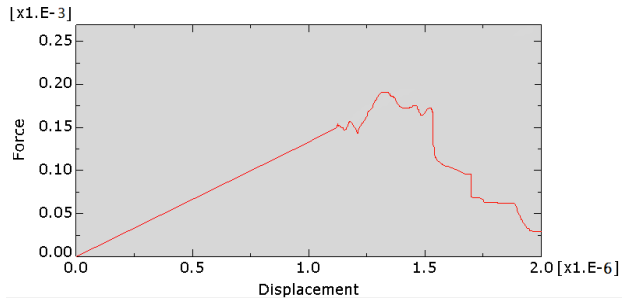

Figure 4.15: Force - amplitude displacement of model 4.1

$$F_{max} = 2e^{-4}N$$

The embedded length, which is the length of the fiber in contact with the matrix, is:

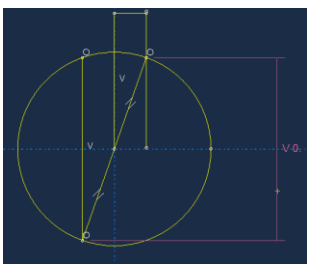

= 9.43980931996518e-05; $l_e \cong 9.43981e^{-5}m$

From table 3; $d_f = 33\mu m = 3.3e^{-5}m$

By substituting those values on the interfacial shear strength formula: we get

$$\tau_{IFSS} = \frac{2e^{-4}N}{\pi * 3.3e^{-5}m * 9.43981e^{-5}m} = 0.02\ MPa$$

Net fiber-epoxy contact surface area

$$A_c = 2\pi r l_e = 2\pi * 9.43981e^{-5} * 3.3e^{-5}m = 9.786e^{-9}m^2$$

Model 4.2: (model 4.1 with void)

The overall embedded length

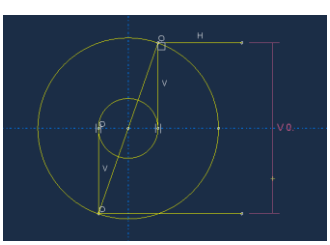

= $9.4398e^{-5}$

gap due to void

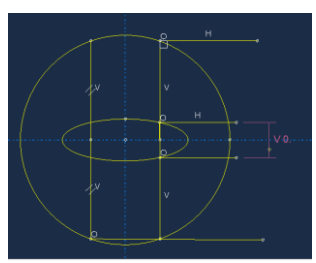

= $1.6732e^{-5} * 2 \cong 3.3464e^{-5}$

The net embedded length is then $9.4398e^{-5} - 3.3464e^{-5} \cong 6.0934e^{-5}m$

$$l_e \cong 6.0934e^{-5}m$$

From table 3:

$$d_f = 33\mu m = 3.3e^{-5}m$$

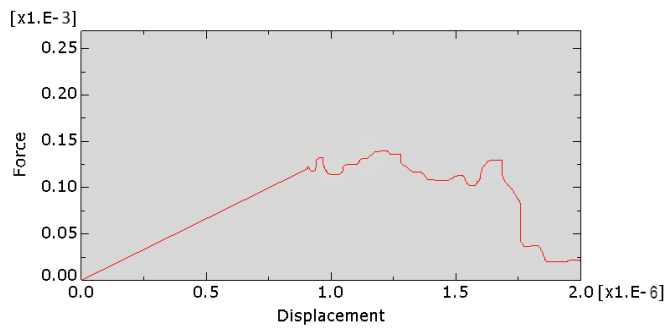

Figure 4.16: Force - amplitude displacement of model 4.2

$$F_{Max} = 0.13e^{-3} = 1.3e^{-4}N$$

By substituting those values on the interfacial shear strength formula: we get

$$\tau_{IFSS} = \frac{1.3e^{-4}N}{\pi * 3.3e^{-5}m * 6.0934e^{-5}m} = 0.0206\ MPa$$

Net fiber-epoxy contact surface area

$$A_c = 2\pi r l_e = 2\pi * 6.0934e^{-5} = 6.32e^{-9}m^2$$

Discussion from the result of models 4.1 and 4.2

For Kapok fiber of 3mm embedded in epoxy, the interfacial area of $9.97e^{-9}m^2$ the Maximum force needed to pull out the fiber is $2e^{-4}\ N$ and the interfacial shear strength is $0.02\ MPa$. While the interfacial contact area decreased by 57.7% to $6.32e^{-7}m^2$ due to the presence of two elliptical voids, the Force also highly decreased by 53.8% to $1.3e^{-3}\ N$ but the IFSS remains the same, only slightly increased by 3% to $0.0206\ MPa$.

- The change in length and the presence of void, change in the area directly proportionally affects the force needed to pull out but that has a negligible effect on the interfacial shear strength.

4.2 The effect of the void

On the pineapple side, on the first model, the presence of void increases the IFSS from 1.393 MPa to 1.43 MPa which is by 2.6%. On the third model, the void increases the IFSS by 1.3% which is from 1.397 MPa to 1.416 MPa. For Kapok, the addition of void on model 5 increased the IFSS by 4.77%, from 0.02 MPa to 0.021 MPa, and by 3% on model 4.1.

4.3 Table of results with corresponding parameters

Table 5: results with changes taken and corresponding parameters and results

Fiber in epoxy	Model no		What is changed?	Max. Force (N)	IFSS (MPa)	Contact interface area (m^2)	Ø (μm)	Length (mm)
Pineapple	1	1.1	–	$6.3e^{-2}$	1.393	$4.52e^{-7}$	48	3
		1.2	The presence of void on 1.1	$5.2e^{-2}$	1.43	$3.62e^{-7}$		
	2	2.1	Changing the embedded fiber length of 1.1	$1.85e^{-2}$	1.397	$1.32e^{-8}$	48	0.1
		2.2	Changing The Ø of 2.1	$1.55e^{-2}$	1.379	$1.124e^{-8}$	36	
		2.3	The presence of void on 2.1	$2.6e^{-2}$	1.4126	$9.56e^{-9}$	48	
		2.4	Changing the void size of 2.3	$1.64e^{-2}$	1.398	$1.16e^{-8}$		
Kapok	3	3.1	–	$2.1e^{-3}$	0.02	$1.04e^{-7}$	33	1
		3.2	The Ø of 3.1	$2.7e^{-3}$	0.0212	$1.27e^{-7}$	45	
		3.3	The presence of void on 3.1	$1.74e^{-3}$	0.021	$8.31e^{-8}$	33	
		3.4	Changing the void size of 3.3	$1.25e^{-3}$	0.022	$5.723e^{-8}$		
	4	4.1	The embedded length of 3.1	$2e^{-4}$	0.02	$9.97e^{-9}$	33	0.1
		4.2	The presence of void on 4.1	$1.3e^{-4}$	0.0206	$6.32e^{-9}$		

Pineapple has interfacial shear strength on average

$$\tau_{IFSS_{Avg}} = \frac{1.393 + 1.43 + 1.397 + 1.379 + 1.4126 + 1.398}{6} = 1.4016 \text{ MPa}$$

And for Kapok

$$\tau_{IFSS_{Avg}} = \frac{0.0212 + 0.022 + 0.02 + 0.021 + 0.02 + 0.0206}{6} = 0.0208 \text{ MPa}$$

By taking the τ_{IFSS} values of all 6 models for each fiber, we got the τ_{IFSS} values 1.4016 MPa and 0.0208 MPa for pineapple and kapok respectively.

In order to see the relation between some of the mechanical properties of the two fibers to the interfacial shear strength results. Those average IFSS values are taken.

Table 6: $\tau_{IFSS_{Avg}}$ of kapok and pineapple concerning some mechanical properties

	Kapok	***Pineapple***
$\tau_{IFSS_{Avg}}$ (MPa)	0.0208	1.4016
Young's Modulus (GPa)	4	71
Poisson's ratio	0.17	0.35
Density (g/cm^3)	0.29	1.07

Taking their IFSS value of two fibers, the relation between IFSS of NFEM and with respect to some of their mechanical properties can be illustrated in graph as:

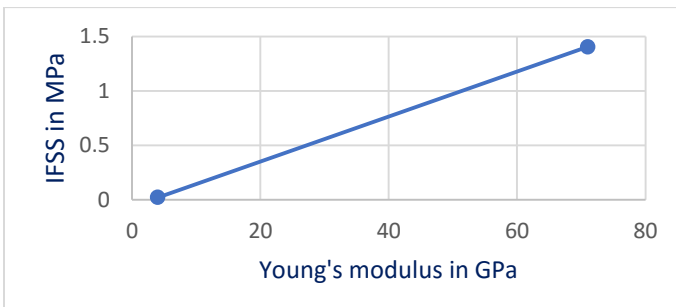

Figure 4.17: Interfacial shear strength of NFEI vs. fiber elasticity

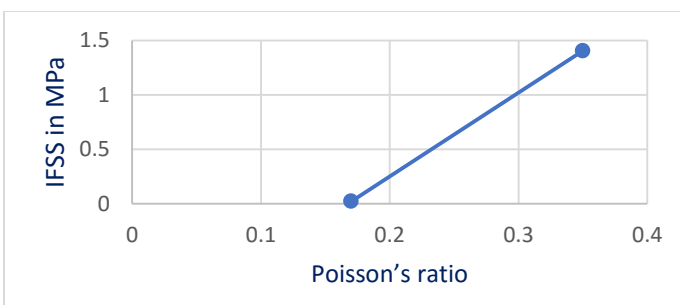

Figure 4.18: Interfacial shear strength of NFEI vs. Poisson's ratio of the fiber

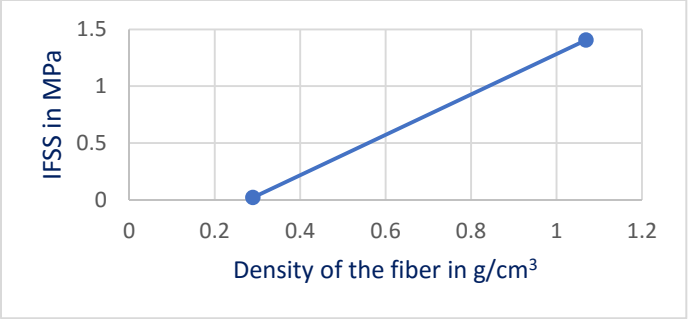

Figure 4.19: Interfacial shear strength of NFEI vs. density of the fiber

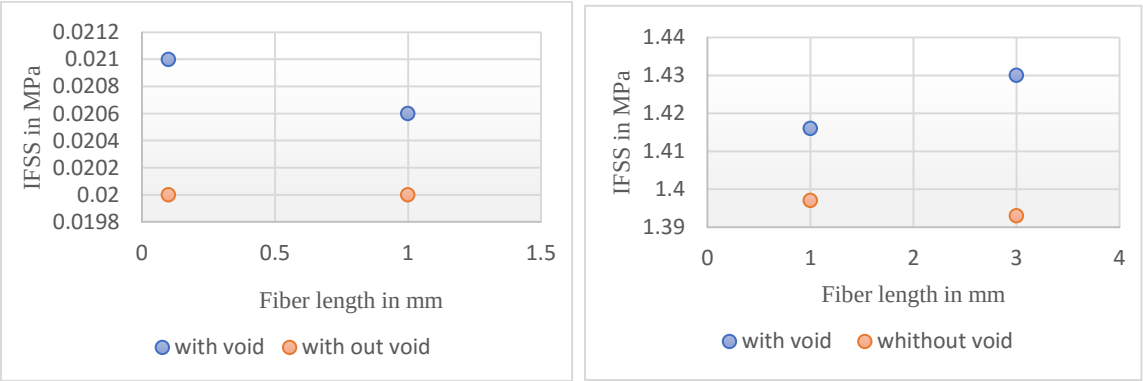

A **B**

Figure 4.20: Interfacial shear strength comparison with change in length and the presence of void of Pineapple (A) and Kapok (B)

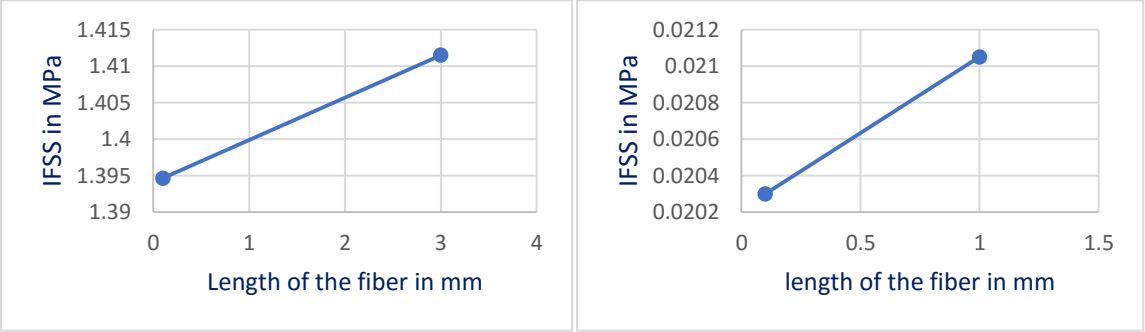

A B

Figure 4.21: Maximum pull-out force vs. epoxy embedded fiber length of Pineapple (A) and Kapok (B)

From the above graph on figure 4.21, we can conclude that the effect of fiber length on the IFSS of NFEM differ with respect to the fiber type, for pineapple the changing the fiber length affects the value of IFSS, i.e for 0.1 mm fiber length, the IFSS value is 1.39465 and for 3 mm EL the IFSS value is 1.4155, so the IFSS increased by 1.495%.

On other hand for kapok changing the EL from 0.1 mm to 1 mm causes the IFSS value to increase from 0.02105 to 0.0203 which is a 3.695% which we can say changing the fiber length do affect kapok that that of pineapple, this is may be related to the difference in the mechanical properties and also diameter of the two fibers.

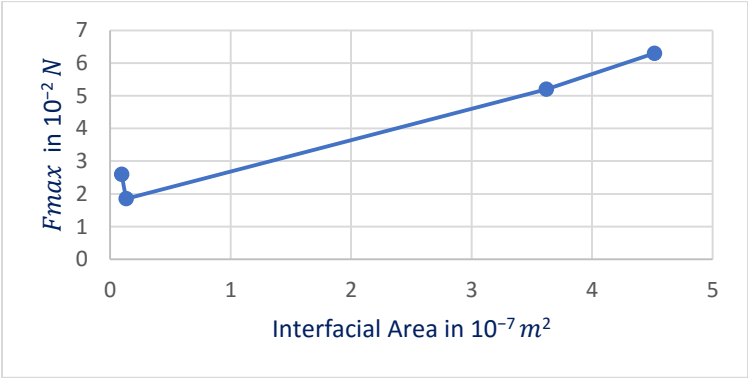

Figure 4.22: Maximum pull-out force vs. fiber-epoxy contact Interface area of Pineapple

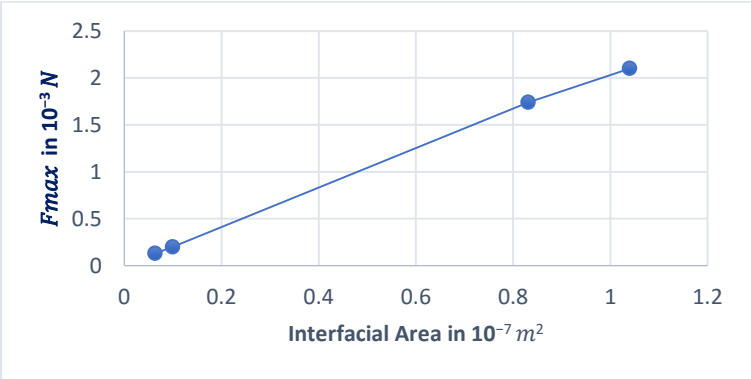

Figure 4.23: Maximum pull-out force vs. fiber-epoxy contact Interface area of Kapok

4.4 Summery

4.4.1 On Pineapple - epoxy matrix

- The change in diameter and length has a negligible effect on the interfacial shear strength of fiber – epoxy matrix.
- The proportionality of the force needed to pull out the fiber and the decrement of interfacial surface area decreases due to void was goes from direct to indirect as the fiber length changes.

4.4.2 On Kapok fiber - epoxy matrix

From the above two summaries and conclusions, it is possible to say

- The change in diameter and length has a negligible effect on the interfacial shear strength of fiber – epoxy matrix.
- The proportionality of the force needed to pull out the fiber and the decrement of interfacial surface area decreases due to void is direct as the fiber length changes.

4.4.3 The effect of void and the effect of change in void

On all models of both natural fibers, the presence of void results in a very small but positive increase of interfacial shear strength. From this we may speculate the presence of more edge on the contact surface of fiber – epoxy matrix, make the fiber a bit hard to pull out because the edge will sack the movement until it deforms to be completely slippery, which will require a relatively high force in contrast to the interface with total smoothness.

4.4.4 The effect of Diameter and fiber length

- The bigger the contact surface area due to length the higher the value of the maximum force required to pull out but the effect of the embedded length nor the contact surface area has **NO** significant effect on the increment or decrement of the interfacial shear strength value but the change in diameter affects IFSS.

4.5 Juxta-positioning results in a variation of additional models

Table 7: Change of IFSS due to change in void ratio and diameter

	Pineapple				**Kapok**			
Change in:	Diameter		Void ratio		Diameter		Void ratio	
model	2.1	2.2	2.3	2.4	3.1	3.2	3.3	3.4
Type of change	Decreasing		Decreasing		Increasing		Increasing	
IFSS	1.397	1.379	1.4126	1.398	0.02	0.0212	0.021	0.022
% difference in IFSS value	-1.3%		-1.0335%		+ 6%		+ 4.76	

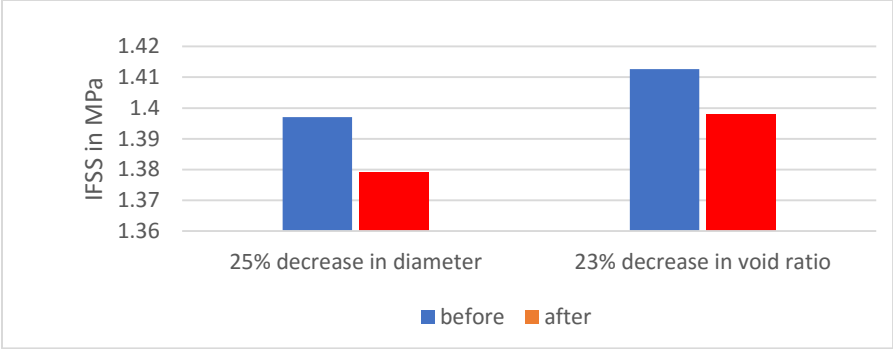

Figure 4.24: Change in IFSS of Pineapple due to change in void ratio

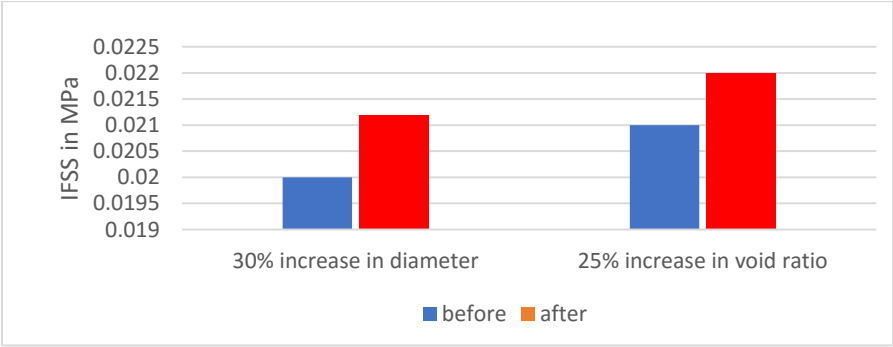

Figure 4.25: Change in IFSS of Kapok due to change in void ratio

- When the diameter of the fiber decreases, the IFSS also decreases
- The presence of void increases the IFSS value

4.6 Comparison with Literature

Table 8: Comparison of IFSS value with literature

Fiber in epoxy	$\tau_{IFSS_{Avg}}(MPa)$	Young's Modulus (GPa)	Poisson's ratio	Density (g/cm^3)
Bamboo	4.91 [59]	27	0.108 [76]	0.616
Kapok	0.0208	4	0.17	0.29
Pineapple	1.4016	71	0.35	1.07
Malva	3.1 [85]	8.8	NA	1.0433 [86]
Jute	2.14 [59]	37.5	0.38 [83]	1.4 [77]

Note: the density of bamboo fiber varies between 0.451 g/cm^{-3} and 0.780 g/cm^{-3} so the average is taken [78].

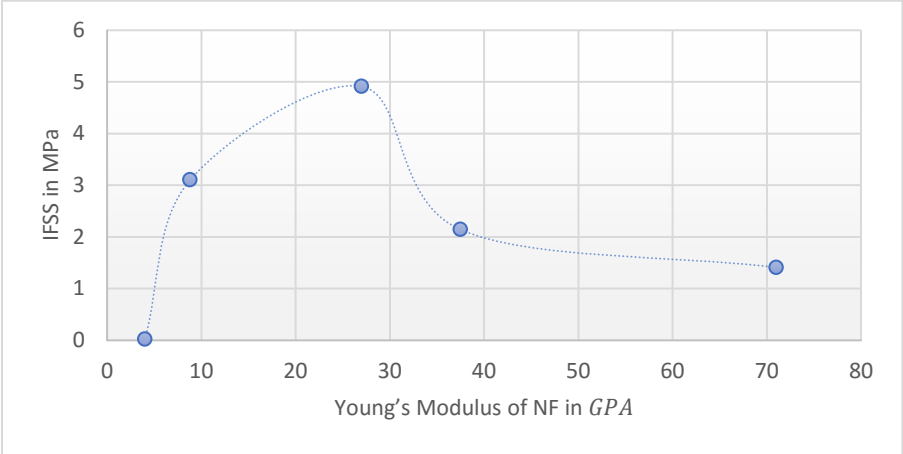

Figure 4.26: The relation between Elasticity of NF and IFSS

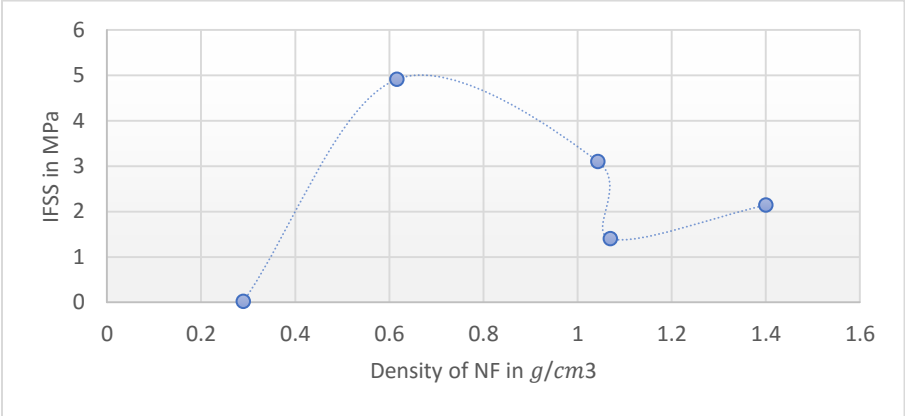

Figure 4.27: The relation of density and IFSS in NFEM

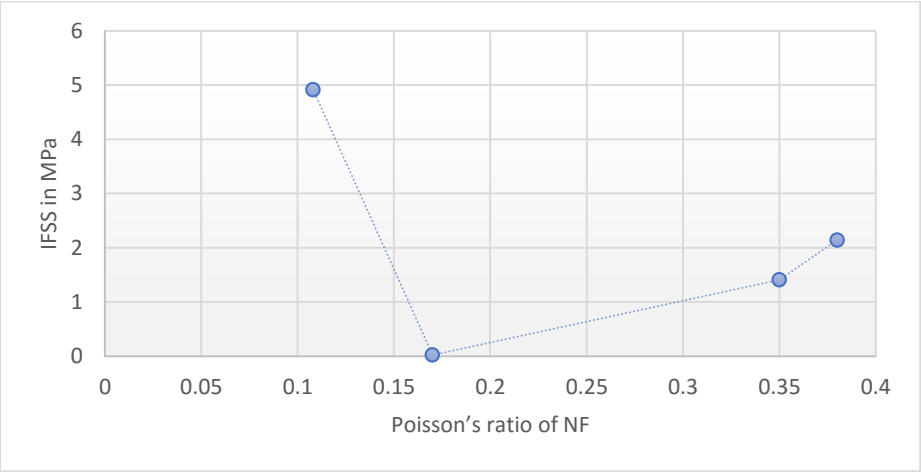

Figure 4.28: Poisson's ratio vs. IFSS of NFEM

Some points regarding the last three graphs:

- From the above graphs, the dependency of IFSS on younger modulus is nearly similar to that of density.
- The curve of IFSS to Poisson's ratio seems to be a mirrored opposite of the relation of IFSS to density and young's modulus.
- There is no linear relation between neither Poisson's ratio, density nor elasticity of the fiber to the interfacial shear strength of NEFM

4.7 Summery regarding the force-displacement graphs

Nearly in all the graphs, the value of force increased constantly, with respect to increase in displacement, to some extent and then starts to fall, from which we sense that the force is applied incrementally until the interface reaches its shear limit and then when the interface becomes fractured the force required in the fiber pulling process will become lessened lesser since the bond in the interface is raptured. But the decrement of the force is not as linear as that of when it was applied before interface fracture, we can speculate that this may be resulted due the presence of some friction, and also the non-uniformity of the interface in shape after breakage and other factors.

5. CHAPTER FIVE: CONCLUSION

5.1 Conclusion

By examining the results and from the discussion made on them, it follows that we can conclude some points as such:

- The shear strength on the interface when pineapple fiber is embedded in epoxy is 1.4016 MPa and when kapok fiber is embedded in epoxy is 0.0208 MPa. For the two fibers, the bigger the young's modulus, density, and Poisson's ratio of the fiber the higher the value of the interfacial shear strength so interfacial shear strength is seemingly dependent on the elastic modulus, Poisson's ratio, and density of the fiber for both kapok and pineapple fiber.
- When comparing the interfacial shear strength result of kapok and pineapple fiber with other natural fiber interfacial shear strength values from the literature. The dependency of IFSS to various mechanical properties is not proportional. More on that the curve of IFSS to density and the curve of IFSS to the elasticity of the fiber looks similar but the curve of IFSS to Poisson's ratio is not similar rather it's proclivity is to be a mirrored opposite.
- The bigger the contact surface area due to length the higher the value of the maximum force required to pull out but the effect of the embedded length nor the contact surface area has no significant effect on the increment or decrement of the interfacial shear strength value but the change in diameter affects IFSS.
- Despite decreasing the contact surface area, the presence of void on the interface has a positive impact on the increment of interfacial shear strength. The decrement of the maximum value of pullout force due to the presence of void is not proportional to the decrement of the net embedded length due to void, so their ratio which determines the value of the interfacial shear strength does not keep in same proportionality when there is void, this may be because of the presence of many internal edges on the surface of the fiber to restrain the pulling-out process so slightly greater force will require for the same embedded fiber length than that of fiber-matrix without void.

5.2 Suggestion

Some of the points to consider in the future work in this area, for better demonstration of IFSS of NFEM and to make it highly related to real world preconditions, are:

- To consider more different fiber orientation and void shaped and angle.
- The effect of change in the mechanical property of the epoxy on the interfacial shear strength is not studied here.
- Including other natural fibers with different mechanical properties is better to characterize the interface the interface of NFEM.
- It is better to do experimental analysis and to compare the values with the numerical one.
- It is better to consider and study the effect of wetness and other environmental factors on the tribology of interfacial shear strength.

REFERENCES

[1] Jacob, M., & Thomas, S. (2008). Biofibers and biocomposites. Carbohydrate Polymers, 71(3), 343-364.

[2]_https://www.concreteconstruction.net/business/technology/natural-fibers-form-eco-friendly-textile-reinforced-concrete_c

[3] Latif, Rashid & Wakeel, Saif & Khan, Noor & Siddiquee, Arshad & Verma, Shyam & Khan, Zahid. (2018). Surface treatments of plant fibers and their effects on mechanical properties of fiber-reinforced composites: A review. Journal of Reinforced Plastics and Composites. Vol. 38. 10.1177/0731684418802022B.C.

[4] Fajrin, J., & Sari, N. H. (2018). Shear properties evaluation of natural fiber reinforced epoxy composites using V-notch shear test. In Matec Web of Conference (Vol. 95, No. 1, pp. 1-7). EDP Sciences.

[5]_https://www.masterclass.com/articles/natural-vs-synthetic-fibers#advantages-of-using-synthetic-fibers

[6] Mechanical behavior of extra-strong CNT fibers and their composites Q.-S. Yang, X. Liu, in Toughening Mechanisms in Composite Materials, 2015.

[7] R. Minty, J. Tomason, and H. Petersen, Te Role of Te Epoxy Resin: Curing Agent Ratio in Composite Interfacial Strength by Single Fiber Micro bond Test,2015.

[8] H.Li, Y.Wang, C.Zhang, and B.Zhang, "Effects of thermal histories on interfacial properties of carbon fiber/polyamide 6 composites: Thickness, modulus, adhesion, and shear strength," Composites Part A: Applied Science and Manufacturing, vol.85, pp.31–39, 2016.

[9] K.M.Beggs, L.Servinis, T.R.Gengenbach, M.G.Huson, B.L. Fox, and L. C. Henderson, "A systematic study of carbon fiber surface grafting via in situ diazonium generatio for improved interfacial shear strength in epoxy matrix composites, "Composites Science and Technology, vol.118, pp.31–38,2015.

[10] B.Liu, Z.Liu, X.Wang, G.Zhang, S.Long, and J.Yang, "Interfacial shear strength of carbon fiber reinforced polyphenylene sulfide measured by the micro bond test, "Polymer Testing, vol. 32, no.4,pp.724–730, 2013.

[11] Leung, C. and V. Li. “Strength-based and fracture-based approaches in the analysis of fiber debonding.” *Journal of Materials Science Letters* 9 (1990): 1140-1142.

[12] GQ Zhang, P Suwatnodom, JW Ju Tongji University, Shanghai, PR China Micromechanics of crack bridging stress-displacement and fracture energy in steel hooked-end fiber-reinforced cementitious composites Volume: 22 issue: 6, November 23, 2012: 829-859.

[13] Victor C. Li, ~ Member, ASCE, and Yin-Wen Chan determination of interfacial debond mode for fiber-reinforced cementitious composites J. Eng. Mech., 1994, 120(4): 707-719.

[14] WJ Cantwell, J Morton (1991). "The impact resistance of composite materials -- a review". Composites. 22 (5): 347–62. doi:10.1016/0010-4361(91)90549-V.

[15] Serope Kalpakjian, Steven R Schmid. "Manufacturing Engineering and Technology". International edition. 4th Ed. Prentice Hall, Inc. 2001. ISBN 0-13-017440-8.

[16] Böhrk, Hannah. (2017). 10 Heat Flux Reduction by Transpiratio-Cooling of CMCs for Space Applications. 10.1515/9783110574432-010.

[17] Sayyar, M., Balachandra, A. M., & Soroushian, P. (2014). The energy absorption capacity of pseudoelastic fiber-reinforced composites. Science and Engineering of Composite Materials, 21(2), 173-179.

[18] https://www.diynaturalbedding.com/product/kapok-fiber/#:~:text=Kapok%20fiber%20is%20the%20seed,foams%20came%20on%20the%20market.

[19] Lim, T. T., & Huang, X. (2007). Evaluation of kapok (Ceiba pentandra (L.) Gaertn.) as a natural hollow hydrophobic–oleophilic fibrous sorbent for oil spill cleanup. Chemosphere, 66(5), 955-963.

[20] Senanurakwarkul, C., Khongsricharoen, P., Pejprom, D., Tantayanon, S., & Khaodhiar, S. (2013). Effects of the composition and the preparatio methods on the oil sorption capacity of recycled rayon waste-kapok mixtures (RRWK) sorbent. International Journal of Environmental Science and Development, 4(3), 246.

[21] Van Tran, A. (2006). Chemical analysis and pulping study of pineapple crown leaves. Industrial Crops and Products, 24(1), 66-74.

[22] https://www.thetextileatlas.com/craft-stories/pina-cloth-philippines

[23] https://www.bagstowear.co.uk/bags-made-from-pineapple-fibersananas-anam/

[24] Tzetzis, D., Tsongas, K., & Mansour, G. (2017). Determination of the mechanical properties of epoxy silica nanocomposites through FEA-supported evaluation of ball indentation test results. Materials Research, 20, 1571-1578.

[25] https://fog.ccsf.edu/~wkaufmyn/ENGN45/Course%20Handouts/14_CompositeMaterials/08_InterfacialStrength.html

[26] Banks-Sills, L. (2015). Interface fracture mechanics: theory and experiment. International Journal of Fracture, 191(1-2), 131-146.

[27] Yang, Q. S., & Liu, X. (2015). Mechanical behavior of extra-strong CNT fibers and their composites. In Toughening Mechanisms in Composite Materials (pp. 339-372). Woodhead Publishing.

[28] Morrell, S. H., & SH, M. (1981). A review of the effects of surface treatments on polymer-filler interactions.

[29] Della Volpe, C., Fambri, L., Fenner, R., Migliaresi, C., & Pegoretti, A. (1994). Air-plasma treated polyethylene fibers: effect of time and temperature aging on fiber surface properties and fiber-matrix adhesion. Journal of materials science, 29(15), 3919-3925.

[30] Beaumont, P. W. (1979). Fracture mechanisms in fibrous composites. In Fracture Mechanics (pp. 211-233). Pergamon.

[31] https://www.twi-global.com/technical-knowledge/faqs/faq-what-is-the-difference-between-debonding-and-delamination-in-adhesive-joints-coatings-and-composites-and-other-defects-found

[32] Daemen, M. J., Ferguson, M. S., Gijsen, F. J., Hippe, D. S., Kooi, M. E., Kevin Demarco, Allard C. van der Wal, Chun Yuan & Hatsukami, T. S. (2016). Carotid plaque fissure: an underestimated source of intraplaque hemorrhage. Atherosclerosis, 254, 102-108.

[33] Safri, S. N. A. B., Sultan, M. T. H., & Jawaid, M. (2019). Damage analysis of glass fiber reinforced composites. In Durability and Life Prediction in Biocomposites, Fiber-Reinforced Composites and Hybrid Composites (pp. 133-147). Woodhead Publishing.

[34] Luo, H. A., & Chen, Y. (1991). Matrix cracking in fiber-reinforced composite materials.

[35] Lamon, J. (2016). Application of Statistical-Probabilistic Approaches to Damage and Fracture of Composite Materials and Structures.

[36] https://www.concrete.org.uk/fingertips-nuggets.asp?cmd=display&id=185

[37] Meng, L., Zhou, B., Ya, B., Jing, D., Jiang, Y., Zhang, D., & Zhang, X. (2020). Microstructures and Properties of AlMgTi-Based Metal-Intermetallic Laminate Composites by Dual-Steps Vacuum Hot Pressing. Materials, 13(18), 3932.

[38] Mouritz, A. P., Chang, P., & Isa, M. D. (2011). Z-pin composites: Aerospace structural design consideratios. Journal of Aerospace Engineering, 24(4), 425-432.

[39] AZIZ, M. (2002). Department of Materials Science and Engineering, Northwestern University, Evanston, IL 60093, USA. Interfaces for the 21st Century: New Research Directions in Fluid Mechanics and Materials Science, 167.

[40] Gope, P. C. (2012). Machine design: Fundamentals and applications. PHI Learning Pvt. Ltd. pp 255.

[41] SRIDHARAN, S., & LI, Y. (2008). Competing cohesive layer models for prediction of delamination growth. In Delamination Behaviour of Composites (pp. 387-428). Woodhead Publishing.

[42] https://abaqus-docs.mit.edu/2017/English/SIMACAEELMRefMap/simaelm-c-cohesiveusage.htm

[43] Papanastasiou, P., & Sarris, E. (2017). Cohesive zone models. In Porous Rock Fracture Mechanics (pp. 119-144). Woodhead Publishing.

[44] Yang, Q. S., & Liu, X. (2015). Mechanical behavior of extra-strong CNT fibers and their composites. In Toughening Mechanisms in Composite Materials (pp. 339-372). Woodhead Publishing.

[45] Krishnan, P. (2019). Evaluation and methods of interfacial properties in fiber-reinforced composites. In Mechanical and Physical Testing of Biocomposites, Fiber-Reinforced Composites and Hybrid Composites (pp. 343-385). Woodhead Publishing.

[46] Packham, D. E. (Ed.). (2006). Handbook of adhesion. John Wiley & Sons. pp 173.

[47] Sørensen, B. F., & Lilholt, H. (2016, July). Fiber pull-out test and single fiber fragmentation test-analysis and modeling. In IOP Conference Series: Materials Science and Engineering (Vol. 139, No. 1, p. 012009). IOP Publishing.

[48] Cantwell, W. J., & Morton, J. (1991). The impact resistance of composite materials—a review. Composites, 22(5), 347-362.

[49] Kalpakjian, S., Schmid, S. R., & Musa, H. (2011). Manufacturing engineering and technology: machining. China Machine Press. 4th Ed. Prentice Hall, Inc. 2001.

[50] https://www.pslc.ws/macrog/mpm/composit/bio/pullout.htm

[51] A. Hodzic, S. Kalyanasundaram, A. Lowe &Z.H. Stachurski The microdroplet test: experimental and finite element analysis of the dependence of failure mode on droplet shape Pages 375 02 Apr 2012.

[52] Meyers, M. A., & Chawla, K. K. (2008). Mechanical behavior of materials. Cambridge university press.

[53] Wang, H., Zhang, X., Duan, Y., & Meng, L. (2018). Experimental and numerical study of the interfacial shear strength in carbon fiber/epoxy resin composite under thermal loads. International Journal of Polymer Science, 2018.

[54] F.-H. Zhang, R.-G. Wang, X.-D. He, C. Wang, and L.-N. Ren, “Interfacial shearing strength and reinforcing mechanisms of an epoxy composite reinforced using a carbon nanotube/carbon fiber hybrid,” Journal of Materials Science, vol. 44, no. 13, pp. 3574–3577, 2009.

[55] P. P. Camanho, C. G. Dávila, and M. F. De Moura, “Numerical simulation of mixed-mode progressive delamination in composite materials,” Journal of Composite Materials, vol. 37, no. 16, pp. 1415–1438, 2003.

[56] M. L. Benzeggagh and M. Kenane, “Measurement of mixed-mode delamination fracture toughness of unidirectional glass/epoxy composites with mixed-mode bending apparatus,” Composites Science and Technology, vol. 56, no. 4, pp. 439–449, 1996.

[57] Dugdale, D. S. (1960). Yielding of steel sheets containing slits. Journal of the Mechanics and Physics of Solids, 8(2), 100-104.

[58] Viel, Q., Esposito, A., Saiter, J. M., Santulli, C., & Turner, J. A. (2018). Interfacial characterization by a pull-out test of bamboo fibers embedded in poly (lactic acid). Fibers, 6(1), 7.

[59] Nahar, S., Khan, R. A., Dey, K., Sarker, B., Das, A. K., & Ghoshal, S. (2012). Comparative studies of mechanical and interfacial properties between jute and bamboo fiber-reinforced polypropylene-based composites. Journal of Thermoplastic Composite Materials, 25(1), 15-32.

[60] Hodzic, A., Kalyanasundaram, S., Lowe, A., & Stachurski, Z. H. (1998). The microdroplet test: experimental and finite element analysis of the dependence of failure mode on droplet shape. Composite Interfaces, 6(4), 375-389.

[61] Friedrich, L. F., & Wang, C. (2016). Continuous modeling technique of fiber pullout from a cement matrix with different interface mechanical properties using finite element program. Latin American Journal of Solids and Structures, 13, 1937-1953.

[62] Zhao, X., He, X. J., Yan, S., & Anh, N. P. (2014). Computational and simulation analysis of pull-out fiber reinforced concrete. Advances in Materials Science and Engineering, 2014.

[64] Zinck, P., Wagner, H. D., Salmon, L., & Gerard, J. F. (2001). Are micro composites realistic models of the fiber/matrix interface? I. Micromechanical modeling. Polymer, 42(12), 5401-5413.

[65] Herrera-Franco PJ and Drzal LT. Comparison of methods for the measurement of fiber/matrix adhesion in composites. Composites 1992; 23: 2–27.

[66] Zhao, Q., Qian, C. C., Harper, L. T., & Warrior, N. A. (2018). Finite element study of the microdroplet test for interfacial shear strength: Effects of geometric parameters for a carbon fiber/epoxy system. Journal of Composite Materials, 52(16), 2163-2177.

[67] Mehdikhani, M., Gorbatikh, L., Verpoest, I., & Lomov, S. V. (2019). Voids in fiber-reinforced polymer composites: A review on their formation, characteristics, and effects on mechanical performance. Journal of Composite Materials, 53(12), 1579-1669.

[68] Mehdikhani, M., Gorbatikh, L., Verpoest, I., & Lomov, S. V. (2019). Voids in fiber-reinforced polymer composites: A review on their formation, characteristics, and effects on mechanical performance. Journal of Composite Materials, 53(12), 1579-1669.

[69] He, S., Wen, Y., Yu, W., Liu, H., Yue, C., & Bao, J. (2017, March). Study on voids of epoxy matrix composites sandwich structure parts. In IOP Conference Series: Materials Science and Engineering (Vol. 182, No. 1, p. 012031). IOP Publishing.

[70] Lim. T.T, Huang. X, Evaluation of kapok (Ceiba pentandra (L.) Gaertn.) as a natural hollow hydrophobic–oleophilic fibrous sorbent for oil spill cleanup Environmental Engineering Research Center, School of Civil and Environmental Engineering, Nanyang Technological University, 50 Nanyang Avenue, Singapore 639798, Republic of Singapore.

[71] Santosh Sadashiv Todkar, Suresh Abasaheb Patil, Review on mechanical properties evaluation of pineapple leaf fiber (PALF) reinforced polymer composites, Composites Part B: Engineering, Volume 174, 2019.

[72] Emad Omrani, Pradeep L. Menezes, Pradeep K. Rohatgi, State of the art on tribological behavior of polymer matrix composites reinforced with natural fibers in the green materials world, Engineering Science and Technology, an International Journal, Volume 19, Issue 2, 2016, Pages 717-736.

[73] Allan F. Bower, Applied Mechanics of Solids, CRC Press, 2009, ISBN: 1439802483, 9781439802489, pp 74.

[74] Xia, Re & Li, Xide. (2008). Mechanical properties testing of kapok fiber and its SiO2 composite. Proceedings of SPIE - The International Society for Optical Engineering. 7375. 110-. 10.1117/12.839242.

[75] https://www.onlinemath4all.com/surface-area-of-prisms-and-cylinders.html

[76] Hua, G., Yang, M., Fei, W., & Lu, F. (2020). Poisson's ratios of molded pulp materials by digital image correlation method and uniaxial tensile test. Journal of Engineered Fibers and Fabrics, 15, 1558925020908271.

[77] Gupta, M. K., & Srivastava, R. K. (2016). Mechanical properties of hybrid fiber-reinforced polymer composite: A review. Polymer-Plastics Technology and Engineering, 55(6), 626-642.

[78] Rusch, F., Ceolin, G. B., & Hillig, É. (2019). Morphology, density and dimensions of bamboo fibers: a bibliographical compilation.

[79] Thyavihalli Girijappa, Y. G., Mavinkere Rangappa, S., Parameswaranpillai, J., & Siengchin, S. (2019). Natural fibers as a sustainable and renewable resource for the development of eco-friendly composites: a comprehensive review. Frontiers in Materials, 226.

[80] Zhao, Q., Qian, C. C., Harper, L. T., & Warrior, N. A. (2018). Finite element study of the microdroplet test for interfacial shear strength: Effects of geometric parameters for a carbon fiber/epoxy system. Journal of Composite Materials, 52(16), 2163-2177.

[81] https://abaqus-docs.mit.edu/2017/English/SIMACAEGSARefMap/simagsa-c-absunits.htm

[82] Feng, G., Kang, Y., & Wang, X. C. (2019). Fracture failure of granite after varied duratios of thermal treatment: an experimental study. Royal Society open science, 6(7), 190144.

[83] Gowda, T. M., Naidu, A. C. B., & Chhaya, R. (1999). Some mechanical properties of untreated jute fabric-reinforced polyester composites. Composites Part A: applied science and manufacturing, 30(3), 277-284.

[84] Shi Meiwu, Xiao Hong, Yu Weidong, September 4, 2009, The Fine Structure of the Kapok Fiber, Volume: 80 issue: 2, pp: 159-165

[85] Margem, J. I., Gomes, V. A., Margem, F. M., Ribeiro, C. G. D., Braga, F. O., & Monteiro, S. N. (2015). Flexural behavior of epoxy matrix composites reinforced with malva fiber. Materials Research, 18, 114-120.

[86] Jean Igor Margem, Noan Tonini Simonassi, Frederico Muylaert Margem, Sérgio Neves Monteiro, Weibull Analysis of Density Malva Fibers With Different Diameters, 2012

[87] Kelly, A., & Tyson, A. W. (1965). Tensile properties of fibre-reinforced metals: copper/tungsten and copper/molybdenum. Journal of the Mechanics and Physics of Solids, 13(6), 329-350.

[88] Mechanical Behavior of Materials,(2009) Cambridge University Press by M.A. Meyers and K.K. Chawlars, Second Edition, Prentice-Hall, Upper Saddle River, NJ, 1999

[89] Medina M, C., Molina-Aldareguía, J. M., González, C., Melendrez, M. F., Flores, P., & LLorca, J. (2016). Comparison of push-in and push-out tests for measuring interfacial shear strength in nano-reinforced composite materials. Journal of Composite Materials, 50(12), 1651-1659.

[90] Andersons, J., Joffe, R., Hojo, M., & Ochiai, S. (2001). Fibre fragment distribution in a single-fibre composite tension test. Composites Part B: Engineering, 32(4), 323-332.

APPENDICES

Mechanical Properties of Different Natural Fibers [3]

Natural fiber	Tensile strength (MPa)	Specific strength	Young's modulus (GPa)	Specific Young's modulus	Failure strain (%)
Abca	12	–	41	–	3.4
Alfa	350	–	22	–	5.8
Bagasse	290	–	17	–	–
Banana	721.5	534.5	29	22	2
Bamboo	575	383	27	18	–
Coir	140.5	122	6	5.2	27.5
Cotton	500	323	8	5.25	7
Curaua	825	–	9	–	7.5
Flax	700	482.5	60	41	2.3
Hemp	530	360	45	30.5	3
Isora	550	–	–	–	5.5
Jute	325	230	37.5	26.5	2.5
Kapok	93.3	300	4	12.9	1.2
Kenaf	743	–	41	–	–
Piassava	138.5	–	2.83	–	5
Pineapple	1020	708.5	71	49.5	0.8
Ramie	925	590	23	15	3.7
Sisal	460	317.5	15.5	–	–

Addis Ababa University

Fasil Henok

fasilhen@gmail.com

2022 G.C